

AFIT/GSO/ENY/95D-02

**ANALYSIS OF GRAVITY-GRADIENT SATELLITE  
ATTITUDE INVERSION**

THESIS  
Jules-Francois D. Desamours  
First Lieutenant, USAF

AFIT/GSO/ENY/95D-02

1996 0118 045

DTIC QUALITY INSPECTED 3

Approved for public release; distribution unlimited

The views expressed in this thesis are those of the author and do not reflect the official policy or position of the Department of Defense or the U. S. Government.

AFIT/GSO/ENY/95D-02

**ANALYSIS OF GRAVITY-GRADIENT SATELLITE**

**ATTITUDE INVERSION**

**THESIS**

Presented to the Faculty of the Graduate School of Engineering

of the Air Force Institute of Technology

Air University

In Partial Fulfillment of the

Requirements for the Degree of

Master of Science

Jules-Francois D. Desamours, B.S. Astronautical Engineering

First Lieutenant, USAF

December 1995

Approved for public release; distribution unlimited

## *Acknowledgements*

I would like to thank my advisor, Dr. Christopher D. Hall, for his guidance, patience, and resourceful insights throughout the development of this thesis. His comprehension and explanation of the physical concepts and dynamics of satellites were of great benefit and utility.

Jules-Francois D. Desamours

## *Table of Contents*

	Page
Acknowledgements . . . . .	ii
List of Figures . . . . .	v
List of Tables . . . . .	vi
Abstract . . . . .	vii
I. Introduction . . . . .	1
1.1 General Issue . . . . .	1
1.2 Scope . . . . .	1
1.3 Specific Problem . . . . .	2
1.4 Methodology . . . . .	2
1.5 Outline of Paper . . . . .	3
II. Background . . . . .	4
2.1 Coordinate Reference Frames . . . . .	4
2.2 Pitch Mounted Momentum Wheel . . . . .	5
2.3 Gravity-Gradient Torques . . . . .	5
2.4 Equilibrium Points . . . . .	6
2.5 Spacecraft Stability . . . . .	8
2.6 Assumptions . . . . .	9
III. Equations of Motion . . . . .	10
3.1 Angular Momentum of Momentum Wheel . . . . .	10
3.1.1 Approximations . . . . .	12
3.2 Angular Momentum of Spacecraft . . . . .	14

	Page
3.2.1 Pitch Axis Coupling . . . . .	16
3.3 Quaternion . . . . .	16
3.4 Pitch Equation . . . . .	19
IV. Analysis of Re-Inversion of Polar BEAR Satellite . . . . .	20
4.1 Cause of Inversion . . . . .	20
4.2 Spacecraft and Momentum Wheel Parameters . . . . .	20
4.3 Re-inversion Simulation . . . . .	23
4.3.1 Momentum Wheel and Torques . . . . .	25
4.3.2 Yaw, Roll, and Pitch Angles . . . . .	25
4.3.3 Quaternion . . . . .	27
V. Analysis of Pitch-Only Motion . . . . .	31
5.1 Methodology . . . . .	31
5.2 Results . . . . .	31
5.2.1 Failure to Invert . . . . .	32
5.2.2 Spacecraft Inversion . . . . .	35
5.3 Pitch Angle Oscillations . . . . .	39
5.3.1 Non-Linear Relationship . . . . .	41
VI. Conclusions and Recommendations . . . . .	51
6.1 Conclusions . . . . .	51
6.1.1 Re-inversion . . . . .	51
6.1.2 Pitch-Only Motion . . . . .	52
6.1.3 Universal Recovery Algorithm . . . . .	53
6.2 Recommendations . . . . .	53
Bibliography . . . . .	54
Vita . . . . .	55

## *List of Figures*

Figure	Page
1. Gravity-Gradient Satellite with Coordinate Reference Frames . . . . .	4
2. Momentum Wheel with Coordinate Reference Frame . . . . .	6
3. Gravity-Gradient Torques Per Body Axis. . . . .	7
4. Quaternions for Pitch Only Rotation . . . . .	18
5. Dynamics of Momentum Wheel . . . . .	22
6. Comparison of Momentum Wheel Dynamics . . . . .	24
7. Momentum Wheel and Torques . . . . .	26
8. Re-Inversion Yaw, Roll, and Pitch Angles . . . . .	28
9. Quaternions for Re-Inversion Process . . . . .	30
10. Lack of Inversion . . . . .	33
11. Pitch Angle During Wheel Despin . . . . .	34
12. Lack of Inversion with Quaternions . . . . .	36
13. Spacecraft Inversion . . . . .	37
14. Spacecraft Inversion with Quaternions . . . . .	38
15. Non-Linear Pitch Oscillation Angle Relationship . . . . .	40
16. Time Until Inversion is Reached Given Wheel Despin Time . . . . .	42
17. Pitch Oscillations about Local Points . . . . .	43
18. Pitch Oscillation and Wheel Despin Time Relationship . . . . .	45
19. Pitch Oscillation and Angular Impulse Relationship . . . . .	46
20. Time Until Inversion and Wheel Despin Time Relationship . . . . .	47
21. Time Until Inversion and Angular Impulse Relationship . . . . .	48
22. Despin Pitch Motion for Wheel Mass Inertia of 0.023 kgm <sup>2</sup> . . . . .	49

*List of Tables*

Table		Page
1.	Results of Pitch Oscillation Angle about Local Inflection Points . . . . .	44



*Abstract*

The purpose of this research is to understand and describe the process by which the 1986 Polar BEAR gravity-gradient research satellite of John Hopkins University/Applied Physics Laboratory achieved an orbital attitude correction (re-inversion) from an inverted orientation through the utilization of its momentum wheel. Understanding this process provides an analytical foundation from which a universal attitude inversion process for other gravity-gradient satellites with similar anomalous motions may be sought and developed.

The equations of motion for a gravity-gradient satellite with a momentum wheel are derived and implemented in FORTRAN for simulation of the dynamics of the spacecraft. Several re-inversion characteristics are observed, in particular, the dynamics about the pitch axis. The resulting observations demonstrate an unexpected non-linear relationship between the oscillation angle of the pitch axis and the despin time of the momentum wheel. This phenomenon depends in part on the size of the momentum wheel compared to that of the spacecraft and on the pitch angle at the time of motor torque application.

# ANALYSIS OF GRAVITY-GRADIENT SATELLITE ATTITUDE INVERSION

## *I. Introduction*

### *1.1 General Issue*

Gravity-gradient satellites are designed to utilize the Earth's gravitational force as a passive method of maintaining Earth-pointing attitude control. For added stability, several devices such as momentum wheels, magnetic rods, and eddy current dampers are included in the satellites. Despite these efforts, some gravity-gradient satellites have experienced extreme deviations from their designed attitudes due to unforeseen phenomena. Correcting these anomalous motions with the devices of the satellites requires an understanding of how and when to utilize them for proper attitude remediation.

### *1.2 Scope*

Although the amount of attitude deviation from designed attitude varies in size and effect, the focus of this research is on the re-inversion of gravity-gradient satellites which have undergone complete attitude inversion. The methods of remediation also vary in technique and efficiency, but only the employment of the momentum wheel as a mechanism for recovery is examined and discussed.

### *1.3 Specific Problem*

An example of a gravity-gradient satellite with extreme motions is the Polar Beacon Experiment and Auroral Research (BEAR) satellite of John Hopkins University Applied Physics Laboratory. In November 1986, the satellite was launched into orbit to measure the properties of the near-earth plasma. However, as it entered its first period of fully sunlit orbit in February 1987, its attitude degraded significantly. The roll, pitch, and yaw angles began oscillating until the satellite finally inverted in May 1987 [4]. Consequently, several attempts to re-invert the satellite were undertaken. The third attempt proved to be successful when the momentum wheel was allowed to despin for an orbit before spinning it back to its maximum spin rate. The torque from the wheel in combination with the pitch rate induced from the despining wheel inverted the satellite and captured it in the desired orientation [5].

### *1.4 Methodology*

In this research, simulation of Polar BEAR's re-inversion is conducted to demonstrate and discuss the process by which it occurred. This provides an analytical foundation of the effects of the momentum wheel on the dynamics of the satellite. A universal attitude inversion process for gravity-gradient satellites is then sought through the analysis of the satellite's motion about the pitch axis only since the pitch angle effectively describes when the satellite is inverted.

### *1.5 Outline of Paper*

The structure of this thesis follows the methodology described above. However, before analyzing the re-inversion of Polar BEAR, background information on gravity-gradient satellites and the gravity-gradient torques that it may experience is presented in Chapter 2. Furthermore, the equations of motion employed to simulate the dynamics of the momentum wheel and the spacecraft are presented in Chapter 3. With the background information and the equations of motion, simulation and analysis of the re-inversion of Polar BEAR are subsequently presented and discussed in Chapter 4. The effectiveness of the momentum wheel as a means of inverting the spacecraft is successfully demonstrated. This permits the development of the universal recovery process in Chapter 5 where the inversion of the spacecraft in the least amount of time and with the least amount of energy expended is sought. The motion of the spacecraft is simplified to that about the pitch axis only and the resulting inversion dynamics are observed and discussed. Chapter 6 of the thesis gives the conclusions and recommendations.

## II. Background

### 2.1 Coordinate Reference Frames

By design, gravity-gradient satellites employ the inverse square law of the Earth's gravitational field as a passive attitude control method. This requires a specific spacecraft attitude orientation where the spacecraft's minimum principal moment of inertia is aligned with the spacecraft's local vertical (yaw axis), the maximum principal moment of inertia is normal to the orbital plane (pitch axis), and the intermediate principal moment of inertia is aligned with the velocity vector of the spacecraft (roll axis) [1]. The orientation of the spacecraft relative to Earth in Cartesian coordinate systems is shown in Figure 1.  $\hat{\mathbf{I}}$  is the

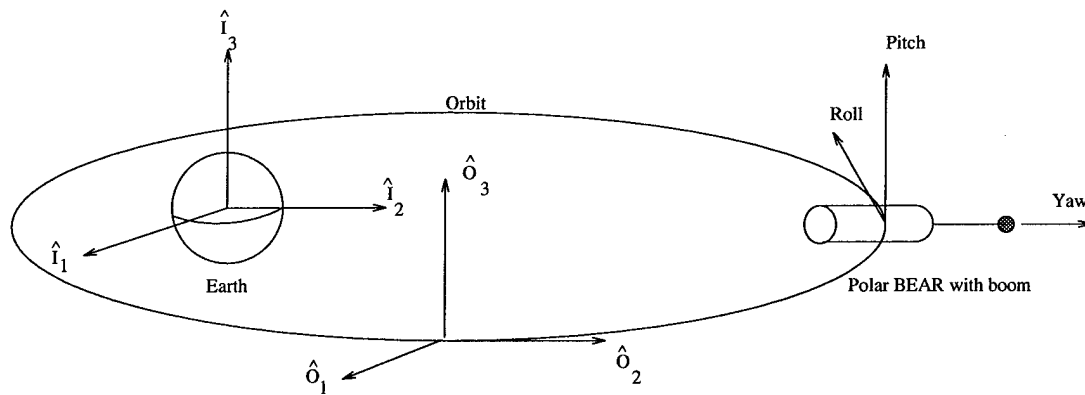


Figure 1. Gravity-Gradient Satellite with Coordinate Reference Frames

inertial reference frame with its origin fixed at the center of Earth and  $\hat{\mathbf{O}}$  is the orbit-fixed reference frame. From the inertial frame,  $\hat{\mathbf{O}}$  rotates about its third axis as it follows the spacecraft along the orbit.  $\langle \text{Yaw}, \text{Roll}, \text{Pitch} \rangle$  represent the body-fixed reference frame of

the spacecraft. Using the right hand rule, positive spacecraft rotation about the yaw axis is a "left turn", roll axis is "left wing up", and pitch axis is "nose down".

## 2.2 *Pitch Mounted Momentum Wheel*

The stability of the spacecraft about the pitch axis is critical for gravity-gradient satellites with earth-pointing accuracy requirements. The environment can impose disturbance torques on the spacecraft, causing oscillatory motions of varying degree about the axes. Since the pitch axis is decoupled from the yaw and roll axes for small angle oscillations, the pitch axis is highly susceptible to disturbance torques [9]. Mounting a momentum wheel with a large angular momentum about the pitch axis provides the gyroscopic stiffness required for that axis. The effects of the disturbance torques are thereby significantly reduced, if not eliminated. Figure 2 shows the coordinate reference of the momentum wheel relative to the spacecraft.  $\hat{a}$  is the axial direction of the momentum wheel relative to the body-fixed frame. For a pitch axis mounted momentum wheel, the components of  $\hat{a}$  in the body frame are  $[0 \ 0 \ 1]^T$ .

## 2.3 *Gravity-Gradient Torques*

The gravitational field of Earth changes in magnitude with altitude. Consequently, the gravitational forces over a body in orbit are not constant, creating gravitational torque about the mass center of the body [2]. The magnitudes of these torques depend on the orientation of the spacecraft to the gravitational field. For Polar BEAR, the gravity-gradient torques per single axis rotation are shown in Figure 3, assuming spherical Earth. Note that the roll and pitch axes

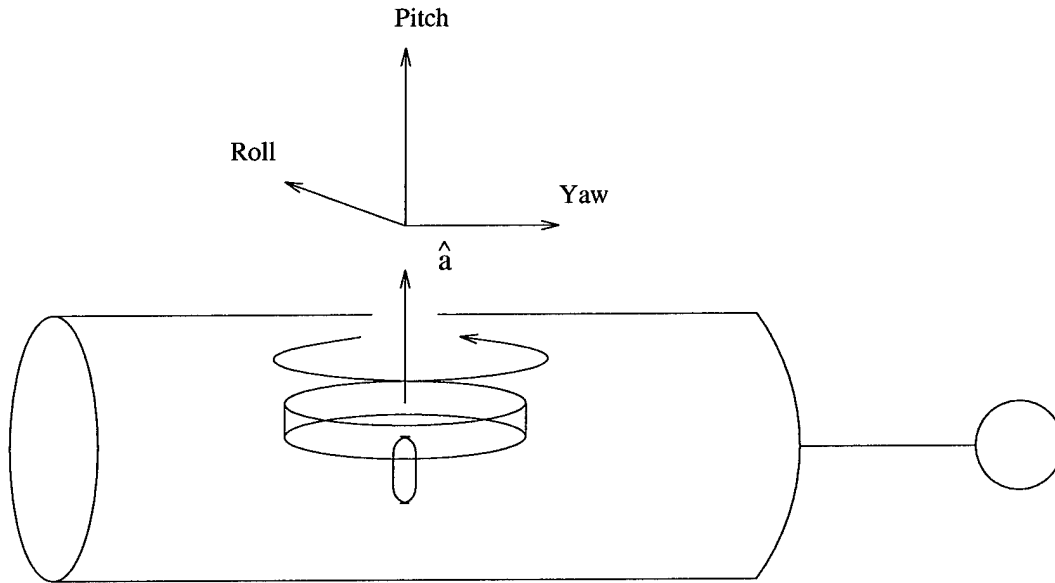


Figure 2. Momentum Wheel with Coordinate Reference Frame

have maximum gravity-gradient torques (0.0013 Nm) at 45° rotation intervals and minimum (zero) torques at 90° rotation intervals. The zero torques (90° rotations) represent either an alignment of the spacecraft with the gravitational field or an orientation where the gravitational forces are uniformly distributed along the body. Neither case induces gravitational torques on the spacecraft. When this occurs, the spacecraft is said to be in an equilibrium configuration. Any deviation from the configuration will induce gravitational torques attempting to restore the spacecraft back to the equilibrium configuration. This in turn induces motion about the axis. Note that any rotation about the yaw axis produces no gravity-gradient torques.

#### 2.4 *Equilibrium Points*

There are 24 equilibrium configurations possible for a gravity-gradient satellite in circular orbit. They are obtained by aligning any of the three principal axes with the orbit

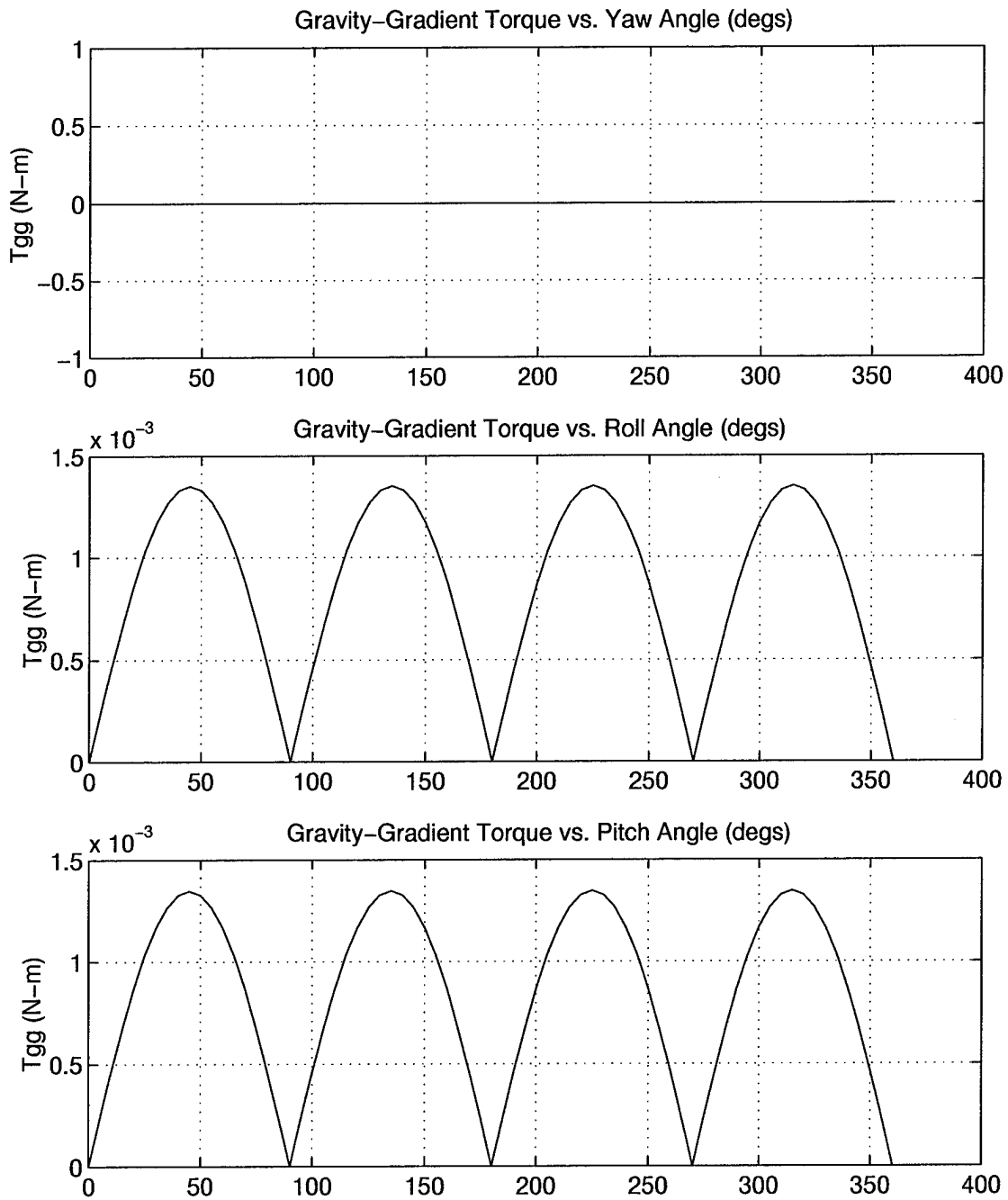


Figure 3. Gravity-Gradient Torques Per Body Axis.



normal and either of the remaining two axes with the local vertical [10]. In other words, rotating any principal axis through 90° intervals provides an equilibrium configuration. This is substantiated by the lack of gravity-gradient torques at 90° rotation intervals as discussed above.

## 2.5 *Spacecraft Stability*

Not all equilibrium orientations are stable. A stable orientation is one where the satellite will not “swing away from the equilibrium point” if the satellite is disturbed [10]. In other words, if the spacecraft is in a stable configuration, it will have stable motions about the equilibrium point. If not, it will completely deviate from that point. Assuming a rigid spacecraft where the momentum wheel is locked (not spinning) with the platform of the spacecraft, then the criteria for pitch stability are

$$B > A \tag{1}$$

$$1 + 3k_1 + k_1k_2 > 4\sqrt{k_1k_2} \tag{2}$$

$$k_1k_2 > 0 \tag{3}$$

where

$$k_1 = \frac{C - A}{B} \tag{4}$$

$$k_2 = \frac{C - B}{A} \tag{5}$$

$A$ ,  $B$ , and  $C$  are principal moments of inertia of the spacecraft along the local vertical, the velocity vector, and the orbit normal, respectively [10]. For example, if Polar BEAR is in the designed orientation, then the values for  $k_1$  and  $k_2$  are 0.97 and 0.10 respectively. All criteria are satisfied, indicating a stable equilibrium configuration. If Polar Bear was rotated by  $90^\circ$  or  $-90^\circ$  about the pitch axis only, then the values for  $A$ ,  $B$ , and  $C$  would change.  $B$  would equate to the minimum spacecraft moment of inertia and  $A$  would equate to the intermediate moment of inertia. This configuration does not satisfy the first criterion, indicating an unstable equilibrium orientation.

## 2.6 Assumptions

Two major assumptions are considered in this simulation. The first pertains to the rigidity of the wheel and the platform of the spacecraft. The wheel and platform are assumed to be a rigid where no structural deformation or change in their center of mass occur. This assumption allows for the development of equations of motion for the rigid platform of the spacecraft given a rigid momentum wheel. The second assumption is that the spacecraft is in a circular orbit about a perfectly spherical Earth.

### III. Equations of Motion

Changing the attitude of a spacecraft requires an adjustment of its angular momentum. This can be accomplished through applied torques or energy dissipation techniques [6]. However, in this simulation, only the applied torque of the momentum wheel on the gravity-gradient satellite is considered. The equations of motion for such a system have been extensively derived in several books, including the book *Spacecraft Attitude Dynamics* by Peter C. Hughes [2]. In this chapter, the equations are presented to illustrate how the momentum wheel is incorporated in the equations of motion of the spacecraft. Furthermore, they are the equations used to do all simulations and obtain the kinematics of the spacecraft.

#### 3.1 Angular Momentum of Momentum Wheel

We begin with the axial angular momentum of the momentum wheel which is defined as

$$h_a = I_w \omega_a \quad (6)$$

where  $I_w$  is the axial moment of inertia of the wheel and  $\omega_a$  is the angular velocity of the wheel about its symmetry axis relative to the inertial reference frame.  $\omega_a$  is composed of the angular velocity of the wheel relative to the platform ( $\omega_w$ ) and the axial component of the angular velocity of the spacecraft relative to the inertial frame ( $\vec{\omega} \cdot \vec{a}$ ):

$$\omega_a = \omega_w + \vec{\omega} \cdot \vec{a} \quad (7)$$

However, to change the angular momentum of the wheel, an external torque must be applied to the wheel [1]. This leads us to the first equation of motion which is the time derivative of the angular momentum of the momentum wheel

$$\dot{h}_a = T_a \quad (8)$$

$T_a$  is the axial torque of the wheel and is composed of the torque from the wheel's motor ( $T_m$ ), the frictional torque ( $T_f$ ), and the gravity-gradient torques ( $T_{gg-wh}$ ).

$$T_a = T_m + T_f + T_{gg-wh} \quad (9)$$

$T_m$  is assumed constant and when applied, produces a torque about the wheel's spin axis which spins up the wheel.  $T_f$  depends on the relative speed of the wheel:

$$T_f = -c\omega_w \quad (10)$$

where  $c > 0$  is the damping constant. If the wheel is not spinning relative to the platform, then there is no frictional torque on the wheel. Conversely, the maximum frictional torque occurs at maximum wheel spin rate.  $T_f$  is negative since it opposes the spin of the wheel.  $T_{gg-wh}$  represents the axial torque on the wheel due to the gravity-gradient field. However, since the wheel is symmetric about its spin axis, no axial gravity-gradient torque is induced on it.

3.1.1 *Approximations.* Given the equation of motion for the momentum wheel, the angular velocity (spin rate) of the wheel at a given time can be approximated. Substituting equation (7) into equation (6) and taking the time derivative of the equation yields

$$\dot{h}_a = I_w(\dot{\omega}_w + \frac{d}{dt}(\vec{\omega} \cdot \vec{a})) \quad (11)$$

However, if the motor is turned off ( $T_m = 0$ ) and the momentum wheel is despinning, then the angular velocity of the spacecraft is small (relative to inertial frame). Therefore, we can assume that

$$\frac{d}{dt}(\vec{\omega} \cdot \vec{a}) \approx 0 \quad (12)$$

which results in

$$\dot{h}_a = I_w \dot{\omega}_w \quad (13)$$

Now substituting equation (9) for equation (13) and solving for  $\dot{\omega}_w$  yields

$$\dot{\omega}_w = -\frac{c}{I_w} \omega_w \quad (14)$$

which is an approximate first order differential equation for the angular velocity of the wheel.

Its solution is a time dependent exponential function

$$\omega_w(t) = \omega_{w_i} e^{-ct/I_w} \quad (15)$$

where  $\omega_{w_i}$  is the initial spin rate of the wheel. Understand that this is an approximation of the momentum wheel during the despin phase.

We can also approximate the spin-up time of the wheel from any initial spin rate. First, by assuming the motor torque is significantly greater than the frictional torque, friction becomes negligible ( $T_f = 0$ ). Thus,  $\dot{\omega}_w$  from equations (9) and (13) yields

$$\dot{\omega}_w = \frac{T_m}{I_w} \quad (16)$$

Integrating equation (16) and solving for the spin-up time of the wheel yields

$$t_{sp} = \frac{I_w}{T_m}(\omega_{w_f} - \omega_{w_i}) \quad (17)$$

where  $\omega_{w_f}$  is the final spin rate of the wheel. Again, this is an approximation of the wheel spin-up time.

With the angular velocity of the despinning wheel at a given time and the amount of time it takes to spin it up, we can approximate the amount of angular impulse expended during the spin-up of the wheel. The angular impulse is defined as the integral of the torque over its application time

$$M = \int_0^{t_{sp}} T_a dt \quad (18)$$

Note, if the wheel torque is applied for a relatively short period of time, then that makes it an impulsive torque. This is significant when analyzing the resulting dynamics of the spacecraft.

However, equation (18) can be re-written as

$$M = T_m t_{sp} - c \int_0^{t_{sp}} \omega_w(t) dt \quad (19)$$

and substituting equation (15) into equation (19) yields

$$M = T_m t_{sp} + I_w \omega_{w_o} (e^{-ct_{sp}/I_w} - 1) \quad (20)$$

where  $\omega_{w_o}$  is the angular velocity of the wheel at the time of spin-up. Observe that the angular impulse is a function of the spin rate of the wheel at the time of motor torque is applied and the duration of its application. Furthermore, the time of motor torque application depends on the amount of time the wheel is allowed to despin.

### 3.2 Angular Momentum of Spacecraft

The second equation of motion is a vector differential equation describing the change in angular momentum of the spacecraft. and is defined as

$$\dot{\mathbf{h}} = -\boldsymbol{\omega} \times \mathbf{h} + \mathbf{T}_{gg} \quad (21)$$

where

$$\boldsymbol{\omega} = (\mathbf{I}_{sp} - I_w \mathbf{a} \mathbf{a}^T)^{-1} (\mathbf{h} - h_a \mathbf{a}) \quad (22)$$

$\mathbf{h}$ ,  $\boldsymbol{\omega}$ , and  $\mathbf{T}_{gg}$  are column matrices containing the components of the angular momentum vector, the angular velocity vector relative to inertial frame ( $\vec{\omega}$ ), and the gravity-gradient torque of the spacecraft respectively.  $\mathbf{I}_{sp}$  is the moment of inertia tensor of the spacecraft with wheel and  $\mathbf{a}^T$  is the transpose of the components of the axial vector  $\vec{a}$ .  $\boldsymbol{\omega}^\times$  is the skewed matrix

$$\begin{bmatrix} 0 & -\omega_3 & \omega_2 \\ \omega_3 & 0 & -\omega_1 \\ -\omega_2 & \omega_1 & 0 \end{bmatrix}$$

As expected, equations (8) and (21) illustrate the relationship between the angular momentum of the wheel as it affects the dynamics of the spacecraft. In equation (8), a torque applied to the wheel changes the angular momentum of the wheel. With the new angular momentum, a change in the angular momentum of the spacecraft is then achieved, equation (21). This relationship is necessary if the momentum wheel is to be utilized as the sole mechanism for attitude recovery. The angular momentum vector is defined as

$$\mathbf{h} = \mathbf{I}_{sp}\boldsymbol{\omega} + I_w\omega_w\mathbf{a} \quad (23)$$

As for  $\mathbf{T}_{gg}$ , it may be shown to be

$$\mathbf{T}_{gg} = 3\omega_o^2\hat{\mathbf{O}}_1^\times(\mathbf{I}_{sp}\hat{\mathbf{O}}_1) \quad (24)$$



where  $\omega_o$  is the constant orbital velocity of the spacecraft, assuming circular orbit [9].

*3.2.1 Pitch Axis Coupling.* An important factor embedded in the equations of motion is the coupling of pitch motion to yaw and roll. This is unlike the linearized equations of motion where the motion of the pitch axis is decoupled from yaw and roll for small angles [9]. In the non-linear equations, the pitch axis depends on both the motion of the yaw and roll angles and on the external torques. This is evident in the equation for the pitch axis in the spacecraft equation of motion

$$\dot{h}_p = (I_{rr} - I_{yy})\omega_r\omega_y + T_{gg-pitch} \quad (25)$$

$I_{rr}$  and  $I_{yy}$  are the axial moments of inertia about the roll and yaw axis respectively.  $\omega_r$  and  $\omega_y$  are the angular velocities of the spacecraft about the roll and yaw axes.  $T_{gg-pitch}$  is the gravity-gradient torque about the pitch axis.

### 3.3 Quaternion

The kinematics of the spacecraft can be described using the Euler axis and Euler angle, which may be combined to define the quaternion. Any body rotating relative to another can be represented by a single angular rotation (Euler angle) about a single fixed axis (Euler axis) [1]. The quaternion is defined as the combination of the Euler vector ( $\vec{\lambda}$ ), and a scalar ( $q_4$ )

$$\vec{q} = \vec{\lambda} \sin \frac{\mu}{2} \quad (26)$$

$$q_4 = \cos \frac{\mu}{2} \quad (27)$$

$\vec{\lambda}$  is the unit vector of the axis of rotation (Euler axis) and  $\mu$  is the rotation angle (Euler angle).

For example, rotating about the pitch axis only means  $\vec{\lambda}$  in matrix form equates to  $[0 \ 0 \ 1]^T$ .

Substituting this into equation (26) yields

$$\mathbf{q} = \begin{bmatrix} 0 \\ 0 \\ \sin \frac{\mu}{2} \end{bmatrix}$$

Since  $q_3$  and  $q_4$  are trigonometric functions, their interaction becomes significant when describing the motion of the spacecraft. For example, if a body is inverted ( $180^\circ$  of rotation) and rotates through  $-180^\circ$  back to zero, then  $q_3$  goes from 1 to 0 and  $q_4$  goes from 0 to 1 (Figure 4). Also, if a body at  $0^\circ$  rotates through  $-180^\circ$ , then  $q_3$  goes from 0 to -1 and  $q_4$  goes from 1 to 0.

Since the quaternion describes the rotation of a body relative to a reference frame, its elements are functions of time. Taking their time derivatives in turn provides us with additional equations of motion describing the kinematics of the spacecraft. They are

$$\dot{\mathbf{q}} = \frac{1}{2}(\mathbf{q} \times \boldsymbol{\omega}_{bo} + q_4 \mathbf{I} \boldsymbol{\omega}_{bo}) \quad (28)$$

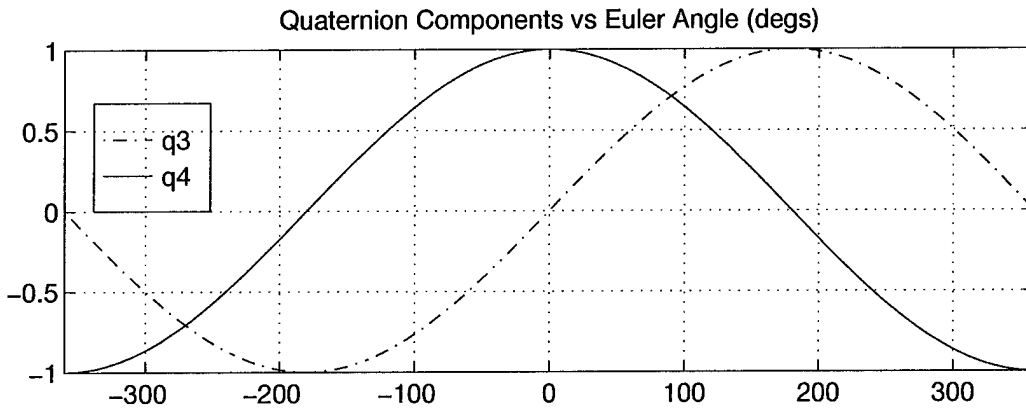
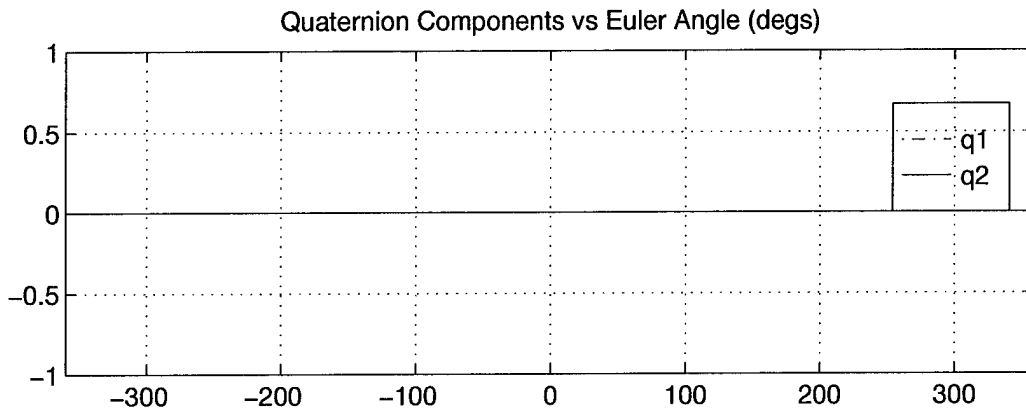


Figure 4. Quaternions for Pitch Only Rotation

and

$$\dot{q}_4 = -\frac{1}{2} \mathbf{q}^T \boldsymbol{\omega}_{bo} \quad (29)$$

where  $\boldsymbol{\omega}_{bo}$  is the column matrix of the components of the angular velocity of the spacecraft with respect to the orbit and  $\mathbf{I}$  is the identity matrix [1].

### 3.4 Pitch Equation

The equations of motion presented above describe the kinematics of the spacecraft in any motion. However, the equation of motion for the pitch angle, assuming motions about the pitch axis only, is defined as

$$\ddot{\theta}_p = \frac{3\omega_o^2(I_{yy} - I_{rr})}{I_{pp} - I_w} \cos \theta_p \sin \theta_p + \frac{T_f}{I_{pp} - I_w} - \frac{T_m}{I_{pp} - I_w} \quad (30)$$

where  $I_{pp}$  is the axial moment of inertia about the pitch axis. Notice that the equation is composed of three terms, each respectively corresponding to the contributions of the gravity-gradient torque, the frictional torque, and the torque of the motor to the dynamics of the pitch angle. This means that no changes to the pitch angle occurs unless one of these torques is in effect.

## *IV. Analysis of Re-Inversion of Polar BEAR Satellite*

### *4.1 Cause of Inversion*

As previously stated, Polar BEAR inverted after experiencing extreme oscillatory motions about all three axes in May 1987 after its first full sun orbit. The specific cause of these anomalous motions remains an unsolved problem to date. Many sources of attitude disturbance such as the Earth's magnetic field, aerodynamic drag, spacecraft charge accumulation, solar radiation pressure, and solar-induced bending of Polar BEAR's boom have been investigated as the potential cause of the inversion. However, neither have been able to substantially produce the instability of the satellite when considered individually. Instead, the subtle accumulation of all environment sources on the spacecraft, working together to overcome the gravity-gradient restoring torques, has been hypothesized. Further analysis of the thermal bending of the boom has also been done, where similar instabilities and anomalous motions were produced. However, the results remain inconclusive [4].

### *4.2 Spacecraft and Momentum Wheel Parameters*

Polar BEAR, in a 1000 km circular orbit, has moments of inertia about the principal yaw, roll, and pitch axes of  $29 \text{ kgm}^2$ ,  $934 \text{ kgm}^2$ , and  $937 \text{ kgm}^2$ , respectively [8]. Its momentum wheel, with an axial moment of inertia of  $0.01137 \text{ kgm}^2$ , provides 2.4 Nms of angular momentum when at its maximum spin rate of 2049 rpm. The spin rate is achieved in approximately 4.5 minutes from zero spin, given a motor torque magnitude of  $0.0093 \text{ Nm}$  [3].

The motor torque was determined using equation (17) and adjusted accordingly given the assumptions of the equation. This demonstrates the overwhelming capability of the motor torque to counter even the maximum gravity-gradient torques of Polar BEAR (0.0013 Nm). Conversely, allowing friction to despin the wheel from maximum spin rate takes approximately 5 to 6 hours [3]. For the re-inversion simulation, a spin-down time of 5.5 hours was chosen to reach a near-zero spin rate of 25 rpm. A near-zero spin is arbitrarily chosen to reduce the amount of time it takes the wheel to reach zero spin since reaching zero spin rate with only viscous damping would take an infinite amount of time (cf. equation (15)). Therefore, the damping constant of the frictional torque to despin the wheel was determined to be  $2.53 \times 10^{-6}$  kgm<sup>2</sup>/s using equation (15). The resulting dynamics of the momentum wheel given these parameters are illustrated in Figure 5.

With the performance of the momentum wheel, the approximations derived in the previous chapter are compared in Figure 6. Observe that the approximations are reasonably close to the actual performance of the momentum wheel. The wheel despins to 25.7 rpm in 330 minutes (5.5 hours) and correspondingly spins up in 4.25 minutes. This results in an expenditure of  $\approx 2.4$  Nms of angular impulse. The close approximations are beneficial when developing a universal recovery process for inverted gravity-gradient satellites. Being able to approximate the dynamics of the wheel helps in determining the minimum requirements for spacecraft inversion, especially in terms of angular impulse. It theoretically represents the amount of energy expended by the motor in order to spin-up the wheel. Inverting the

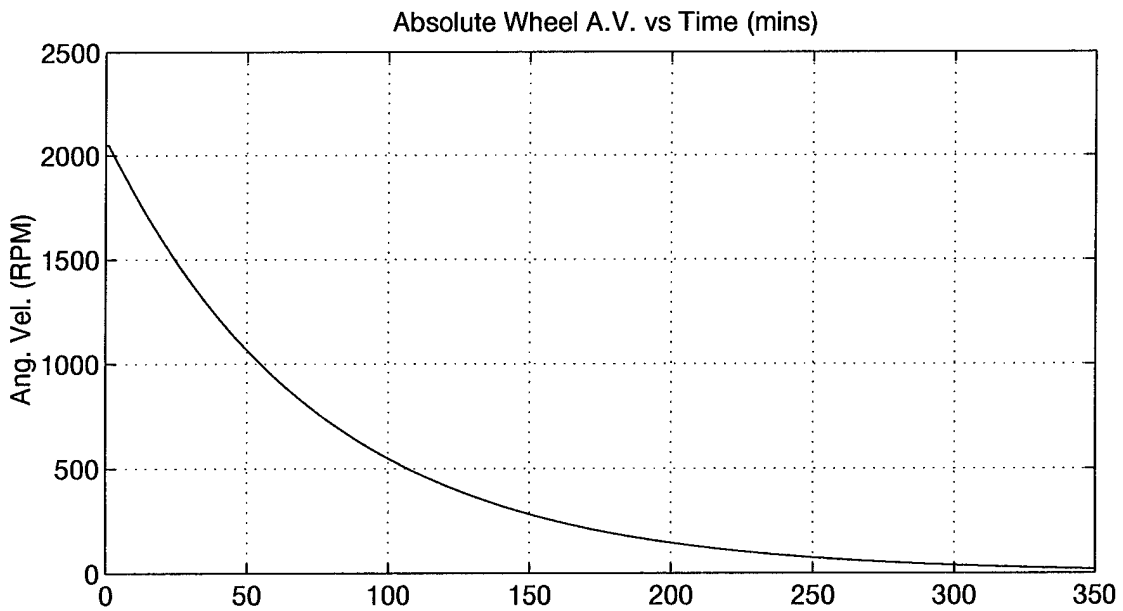
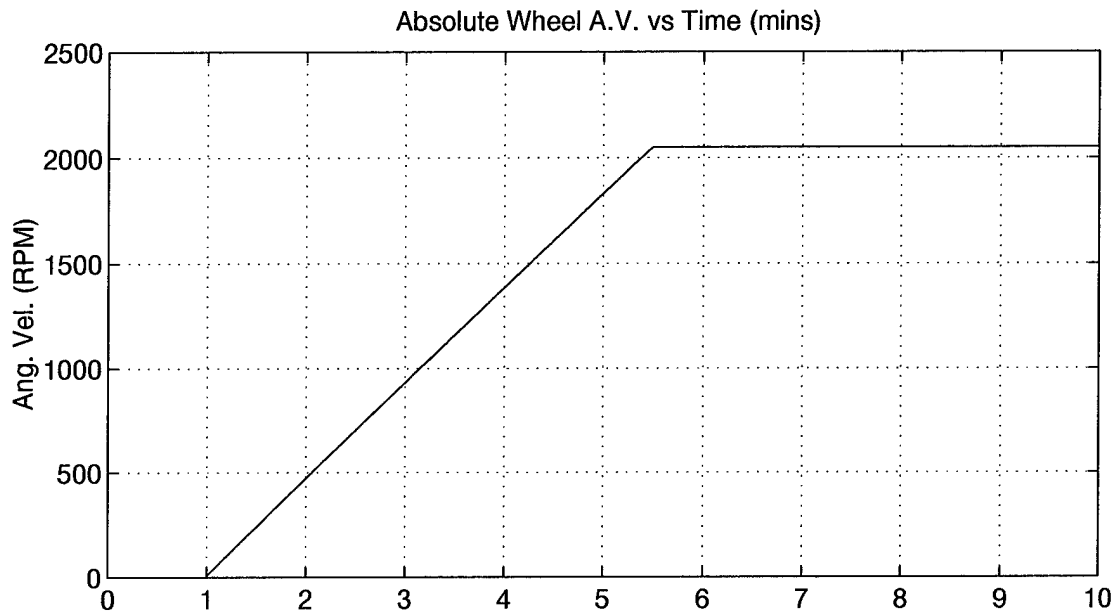


Figure 5. Dynamics of Momentum Wheel

spacecraft with the least amount of angular impulse would be required considering the limited amount of energy available in a satellite.

#### 4.3 *Re-inversion Simulation*

The re-inversion simulation begins with the inverted orientation of the spacecraft at the time of the third attitude correction attempt:  $-10^\circ$ ,  $-20^\circ$ , and  $-180^\circ$  for the yaw, roll, and pitch angles respectively [5]. The motor is turned off for one satellite orbit to despin the wheel from maximum spin rate. The motor is then turned back on, spinning the wheel back up until it reaches spin-up saturation and remains spinning at its maximum spin rate. This is modelled by equating the torque on the wheel ( $T_a$ ) to zero once maximum spin rate is achieved.

It is important not to confuse the wheel spin-up saturation as an absorption of the energy generated by the motor torque. The forces of the motor torque remain constant until the motor is turned off. It is the increase in frictional torque as the wheel spins up that eventually equates to the motor torque and causes saturation. The frictional forces do not absorb or dissipate the motor torque. Without any devices or mechanisms to absorb or dissipate the motor torque, the resulting motions of the spacecraft would continue endlessly [6]. For example, if the motor torque caused the spacecraft to spin (or oscillate) about an axis, it would continuously spin (or remain in oscillatory motions) for an infinite amount of time. The lack of motion damping devices or energy dissipation mechanisms to absorb the energy generated by the motor torque causes the resulting motions to continue. These dynamics are expected in the re-inversion simulation since energy absorption or dissipation is not modelled.



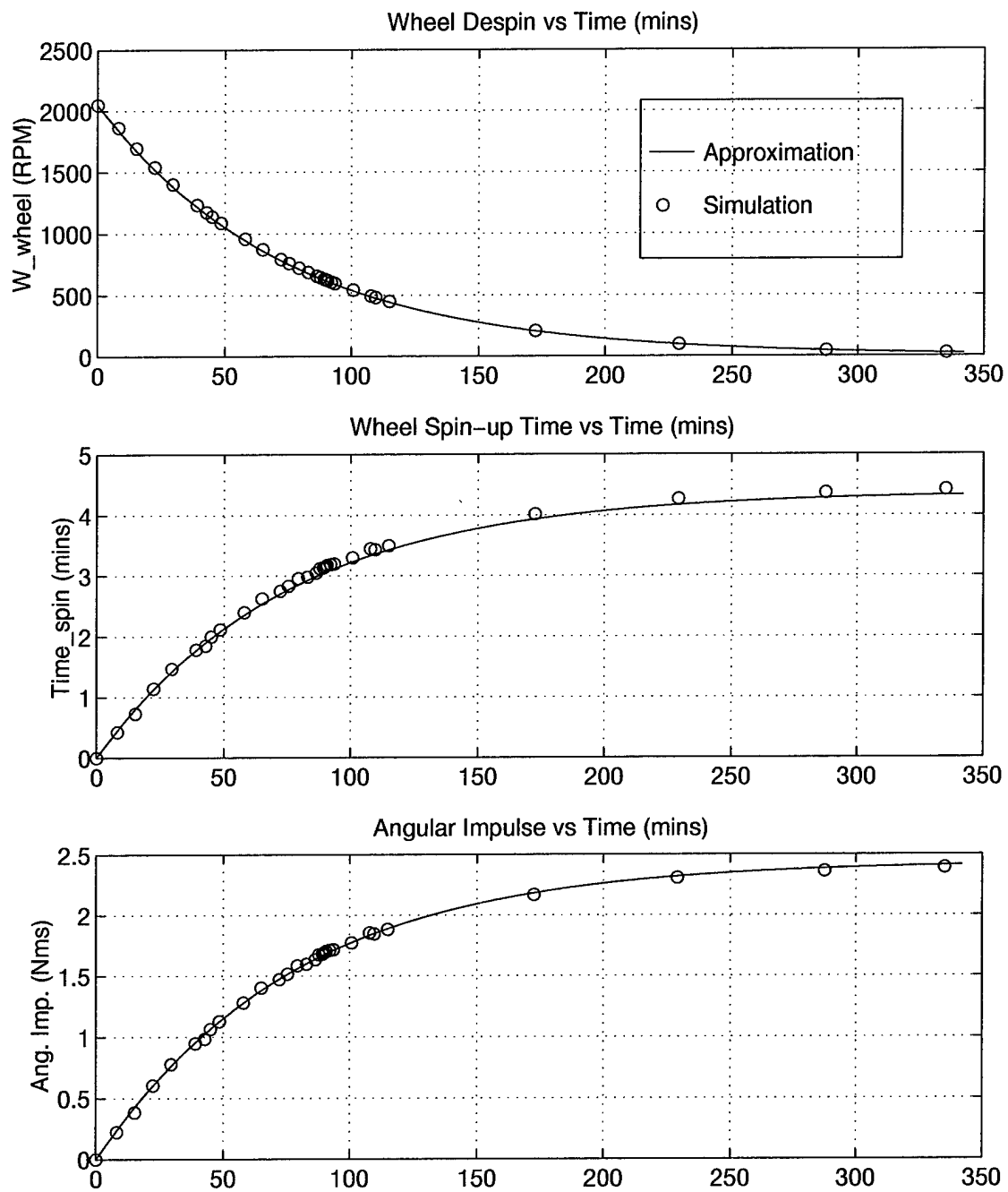


Figure 6. Comparison of Momentum Wheel Dynamics

*4.3.1 Momentum Wheel and Torques.* The dynamics of the momentum wheel and of the torques during the re-inversion process are illustrated in Figure 7. In the first two plots, the wheel despins to  $\approx 450$  rpm where only the frictional torque acts on the wheel. Observe that during the spin-up phase, the torque on the wheel is applied for a relatively short period of time. This short time span makes the application wheel torque an impulsive torque as discussed earlier and expends approximately 1.67 Nms of angular impulse.

The third plot shows the gravity-gradient torques experienced by Polar BEAR during the re-inversion process. The inverted configuration of the spacecraft induces restoring gravity-gradient torques throughout the process. Note that no gravity-gradient torques exist at approximately 138 minutes into the re-inversion process which can only occur at rotation intervals of  $90^\circ$ . The corresponding spacecraft orientation is examined in the next section. The last plot illustrates the torque difference of the torque on the wheel and the restoring torques. It affirms the overwhelming capability of the motor over any other external torque on the satellite.

*4.3.2 Yaw, Roll, and Pitch Angles.* The dynamics of the spacecraft about the three axes during the re-inversion process are illustrated in Figure 8. Recall that any spacecraft deviation from its equilibrium configuration induces gravity-gradient torques and subsequently creates motion about that axis. This justifies the oscillatory motions of the yaw and roll angles induced from their initial inverted angles. These motions continue and do not dampen to within specifications since motion damping devices (such as the eddy current dampers of

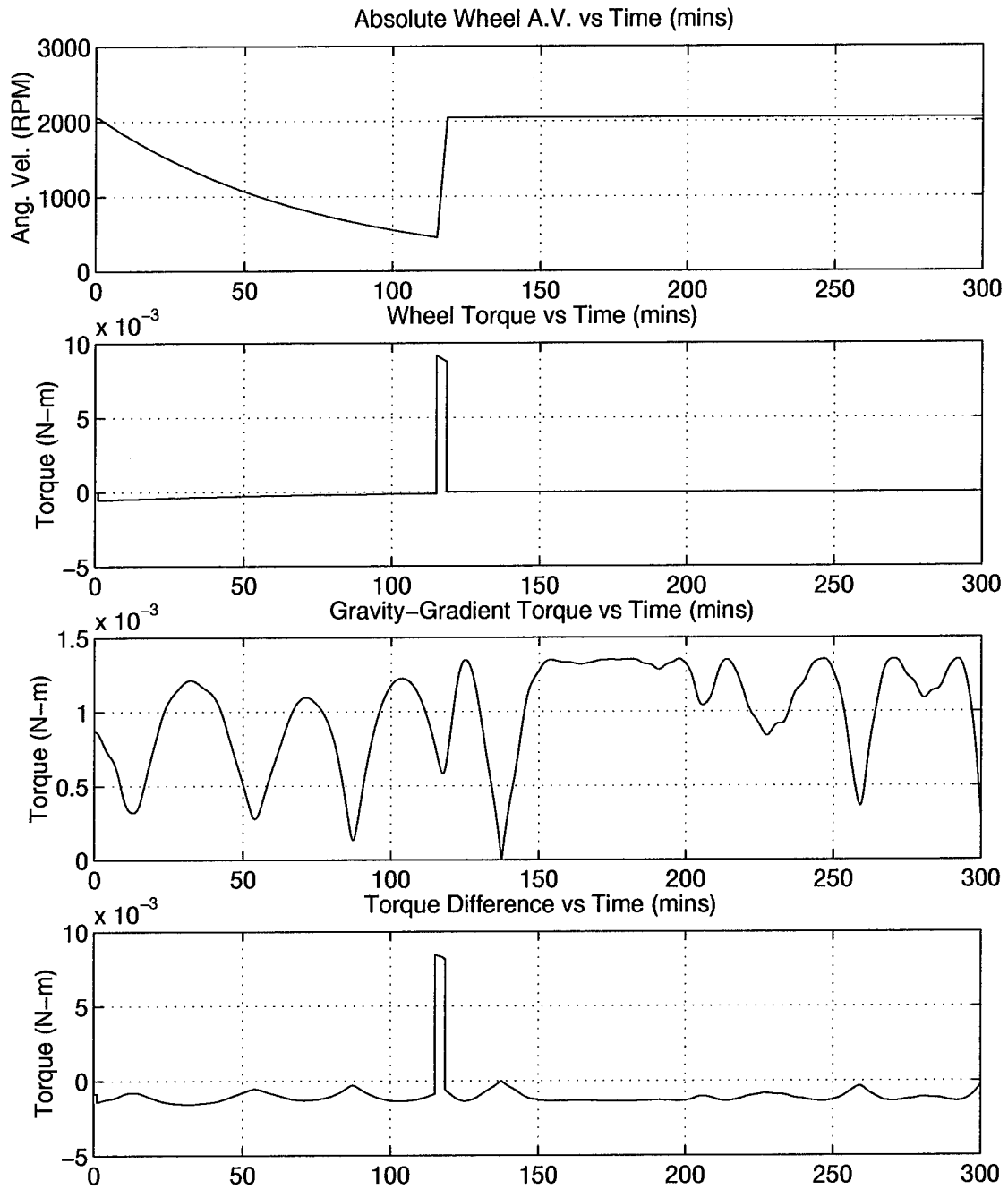


Figure 7. Momentum Wheel and Torques

Polar BEAR) are not modelled in the simulation. In actuality, Polar BEAR dampened to within 10 degrees of mission specifications for all three axes [5].

The pitch angle, although at an inverted equilibrium point initially, produced uneven motions during the despin of the momentum wheel. These motions are the results of the motions of the yaw and roll angles coupled with the pitch axis and of the frictional torque during wheel despin. However, after motor torque application, the pitch axis decreased to  $\approx -400^\circ$  before settling in an oscillatory motion about  $-360^\circ$ . This is a complete inversion of the spacecraft about its pitch axis where the decrease in pitch angle is indicative of a negative rotation about the axis. As expected, the positive motor torque about the pitch axis produced an opposing frictional torque on the spacecraft which in turn generated a negative rotation. Furthermore, the pitch angle stabilized about  $-360^\circ$  instead of continuously decreasing given the lack of energy dissipation in the simulation. The lack of continuous spacecraft spin is attributed to the coupled motions of yaw and roll with the pitch angle.

Observe that at 138 minutes, the yaw, roll, and pitch angles are approximately  $41^\circ$ ,  $-28^\circ$ , and  $-262^\circ$  respectively. This was not previously identified as an equilibrium configuration, where zero gravity-gradient torques exist. However, if the rotation angle ( $\mu$ ) is at a  $90^\circ$  rotation multiple at 138 minutes, then this spacecraft orientation is in some form of an equilibrium configuration. This is examined in the next section.

*4.3.3 Quaternion.* As previously stated, the re-inversion process can be described using the Quaternion (Figure 9). For this case,  $q_1$  and  $q_2$  induced oscillatory motions which indicates and affirms that the rotation of the spacecraft was not solely about the pitch axis.

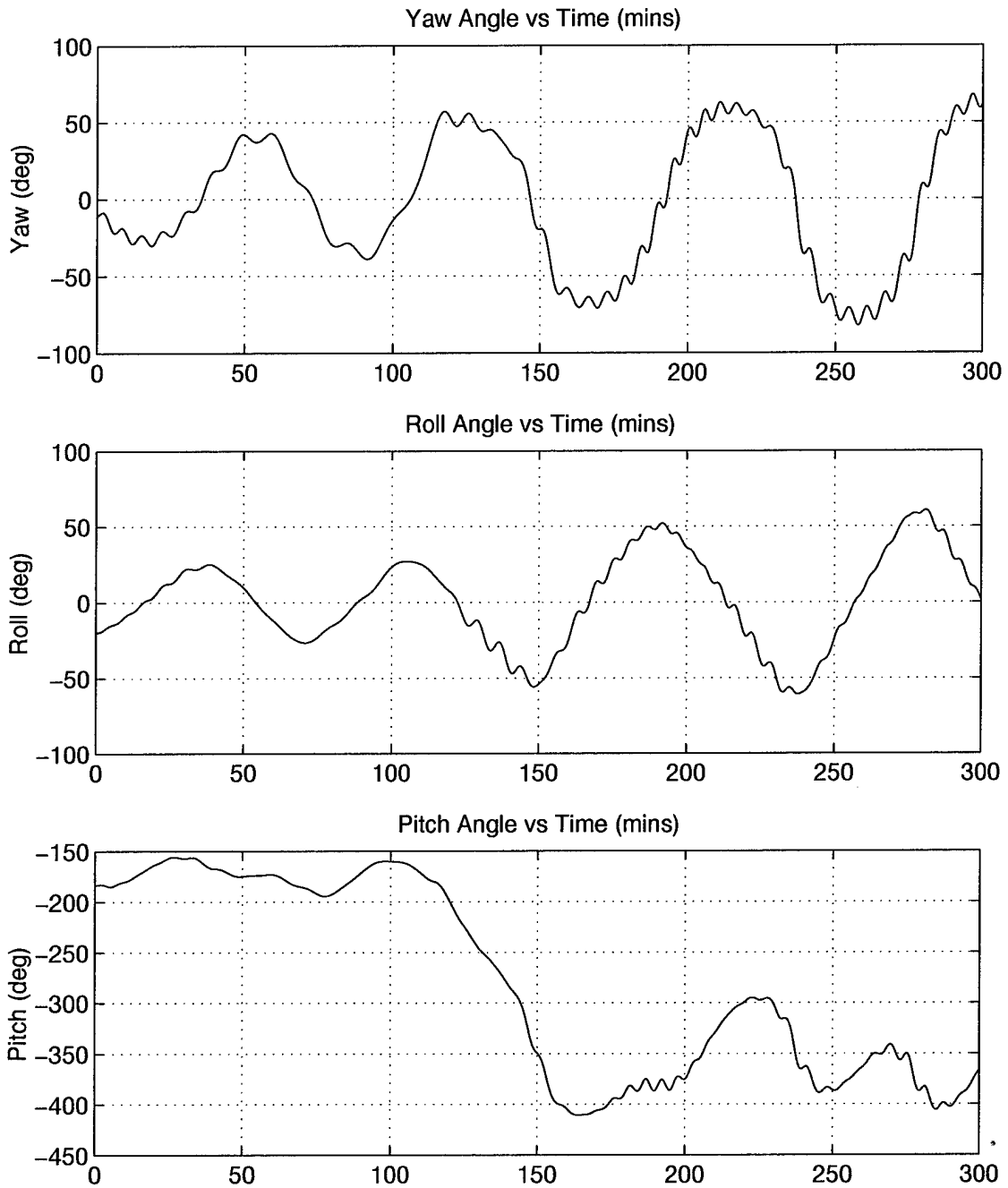


Figure 8. Re-Inversion Yaw, Roll, and Pitch Angles

However, the re-inversion of the spacecraft is seen through the interactions of  $q_3$  and  $q_4$ .  $q_3$  begins at 1 until it decreases and oscillates about 0. Similarly,  $q_4$  begins at 0 and increases to  $\approx 1$ . These interactions describe  $\approx -180^\circ$  of rotation about the pitch axis as expected from the dynamics of the pitch angle as discussed in Chapter 3.

As for the Euler rotation angle  $\mu$ , it begins at  $180^\circ$  of rotation, corresponding to the inverted position of the satellite. It then decreases to  $\approx 60^\circ$  by the end of the inversion. This again demonstrates the combined rotation of the spacecraft about all three axes. If the rotation was solely about the pitch axis,  $\mu$  would decrease to  $0^\circ$ . Furthermore, note that at 138 minutes,  $\mu$  is  $90^\circ$  of rotation. This corresponds to the lack of gravity-gradient torques which indicates the rotation of the spacecraft through an equilibrium configuration.

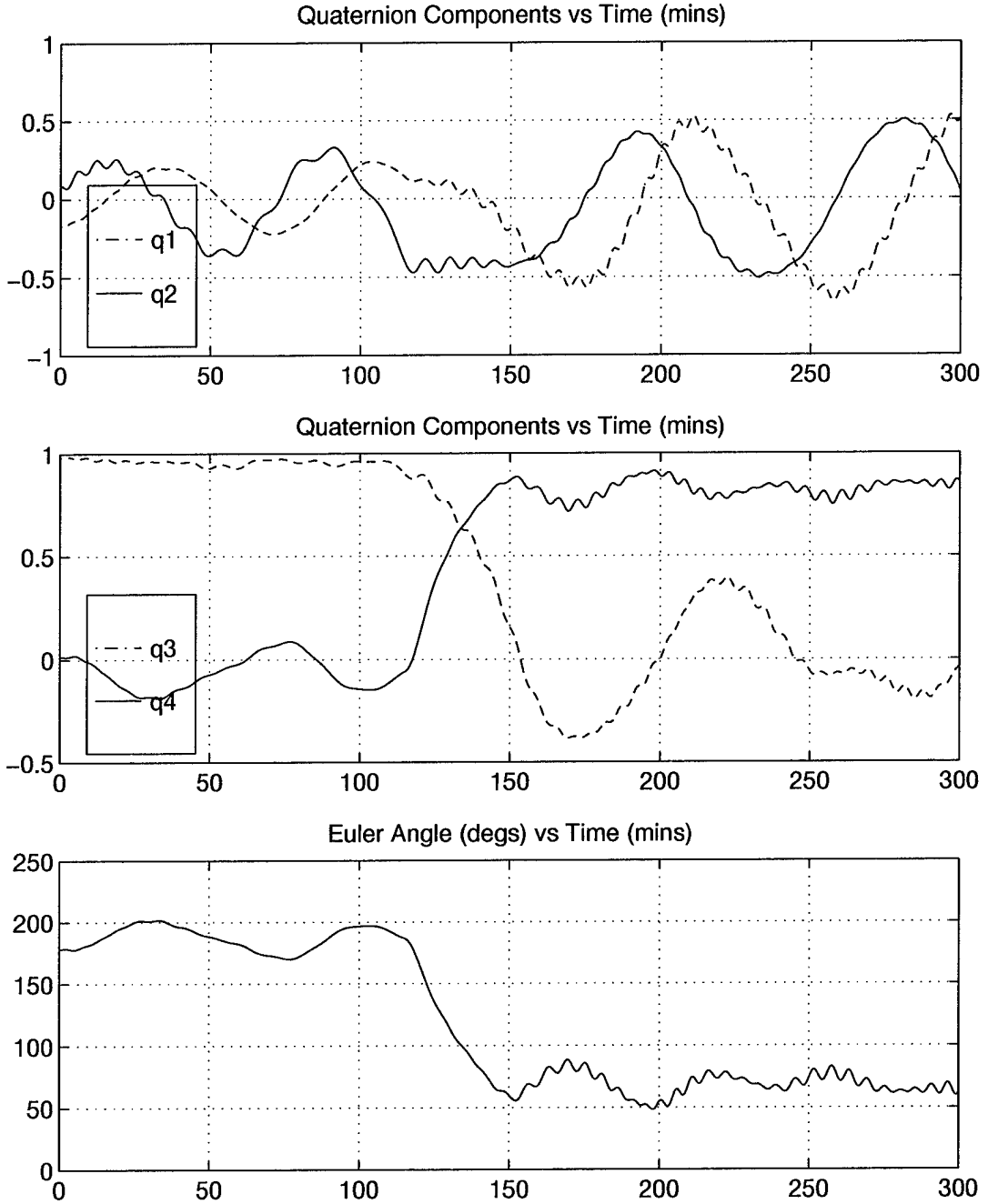


Figure 9. Quaternions for Re-Inversion Process

## *V. Analysis of Pitch-Only Motion*

Having analyzed the re-inversion process, development of an optimal recovery process for inverted gravity-gravity satellites is developed by initially simplifying the spacecraft's motion. The analysis is simplified to motions about the pitch axis for two reasons: the pitch-mounted momentum wheel primarily affects the dynamics of the pitch axis and the pitch angle effectively describes when the spacecraft is inverted. Of specific interest is the amount of time required to despin the momentum wheel in order to invert the spacecraft in the shortest amount of time and with the least amount of energy expended.

### *5.1 Methodology*

The orientation of the spacecraft begins with all three axes at  $0^\circ$  of rotation, which is a stable equilibrium configuration. The momentum wheel despins from its maximum spin rate for a specified amount of time before application of the motor torque. Gradually the despin time is increased until satellite inversion is achieved. The dynamics are then observed for any relationship which may lead to a universal recovery algorithm and formula.

### *5.2 Results*

The inversion of the spacecraft was not achieved in all inversion attempts even though the torque of the motor was greater than the maximum restoring torques as discussed earlier. Evidently, the overwhelming magnitude of the motor torque is not exclusively sufficient of a criteria to invert the spacecraft. Other factors must be involved.



*5.2.1 Failure to Invert.* An example of the spacecraft not inverting occurs when the wheel is allowed to despin for 87 minutes only (Figure 10). Beginning with the despin phase, we see the frictional torque of the motor causes oscillatory motions about the pitch axis where the center of oscillation is offset by  $10^\circ$  from the original equilibrium point ( $0^\circ$ ). This is expected since the continuous application of a torque about an axis will initially offset the oscillation center to a new equilibrium angle. The location of the new center is where the frictional torque and the gravity-gradient torque are of equal magnitude. Recall that the pitch equation, (30), is a function of the frictional torque and the gravity-gradient torque (for zero motor torque). However, as the frictional torque decreases due to the despinning wheel, the location of the oscillation center gradually returns back to the original point. This is illustrated in Figure 11 where the wheel is allowed to despin for a longer time and the oscillations eventually return to oscillate about  $0^\circ$ . Observe also that the first set of negative pitch angles occurs between 52.8 and 75.2 minutes where the pitch angle is  $\approx 0^\circ$  at these times. This becomes relevant in a later discussion of the results.

In the lack of inversion example, we also see the pitch angle oscillating between  $86.7^\circ$  and  $-86.7^\circ$  after the motor torque is applied. These oscillations occurred instead of the inversion of the spacecraft. Again, these motions induced by the impulsive torque on the wheel can be expected. An impulsive torque will produce oscillations about the current center (which may be the original equilibrium point) unless it is large enough to oscillate (or rotate the spacecraft) through the  $90^\circ$  of rotation equilibrium orientation [7]. Recall that the equilibrium orientation with the pitch angle at  $90^\circ$  of rotation is an unstable configuration. Therefore,

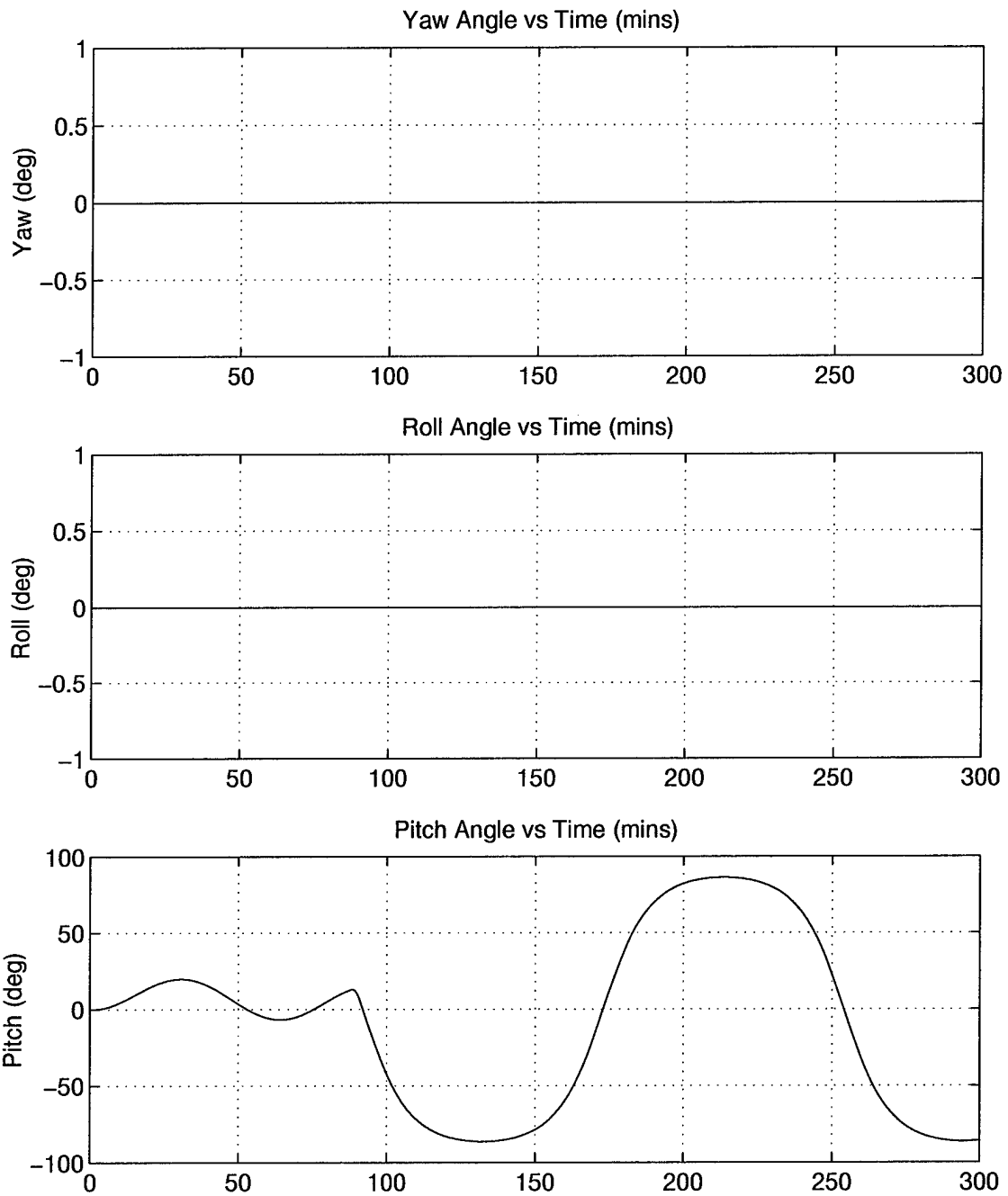


Figure 10. Lack of Inversion

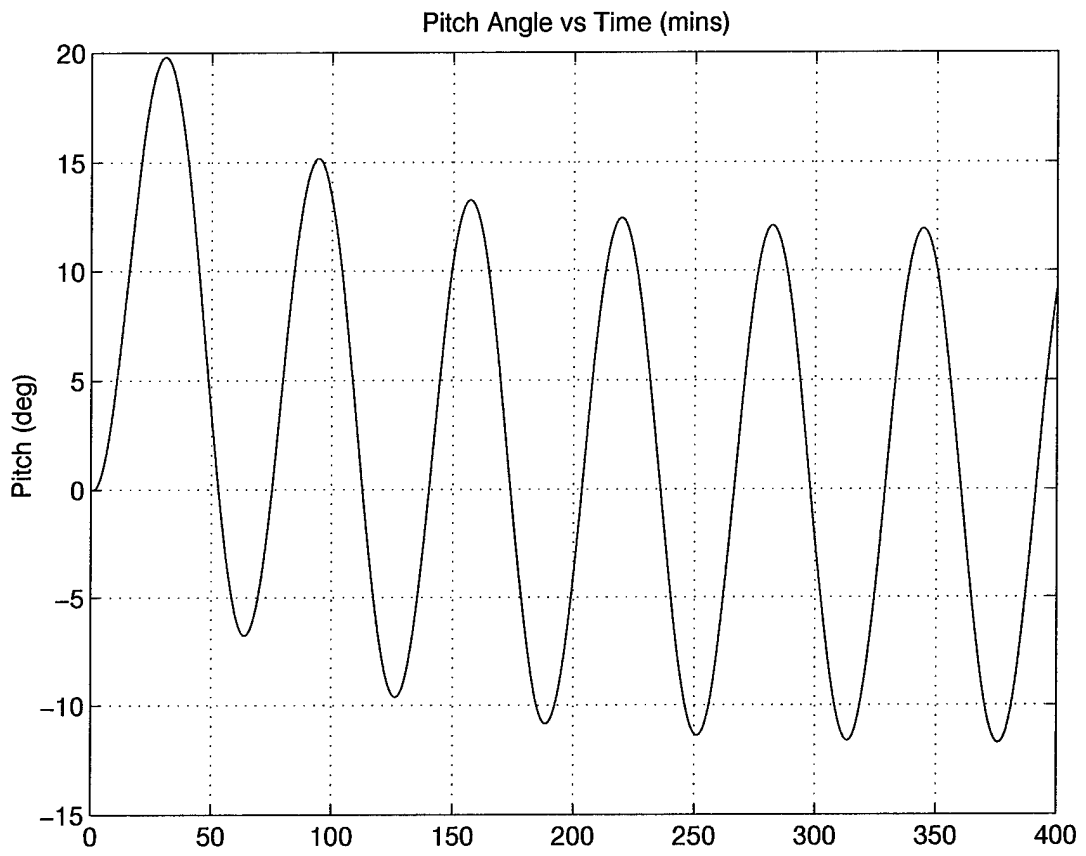


Figure 11. Pitch Angle During Wheel Despin

spacecraft inversion requires an impulsive torque of enough magnitude to pass the spacecraft through the unstable configuration. Otherwise, the spacecraft will only oscillate to within  $90^\circ$  and about the current oscillation center. Determining the required amount of impulsive torque, or the corresponding amount of angular impulse from the wheel, is the basis of the recovery process. Recall also that Polar BEAR similarly rotated through an equilibrium configuration during its re-inversion process, although it was not established as an unstable one.

The lack of inversion is also equivalently illustrated with the quaternions (Figure 12). After the motor was turned on, the Euler angle reached  $86.7^\circ$  of rotation periodically. Observe that  $q_3$  and  $q_4$  are  $-0.686$  and  $0.686$  respectively at the first  $86.7^\circ$  of rotation. This corresponds to  $\approx -90^\circ$  of rotation about the pitch axis as discussed in Chapter 3. Recall that  $q_3$  and  $q_4$  are  $-0.7071$  and  $0.7071$  respectively if a body rotates  $-90^\circ$  about the pitch axis only.

*5.2.2 Spacecraft Inversion.* Letting the momentum wheel despin for one additional minute results in the inversion of the spacecraft (Figure 13). The same dynamics occur for the pitch axis during the wheel despin phase, but after the motor torque is applied, the pitch angle decreases continuously. This represents an inversion of the spacecraft ( $-180^\circ$  of rotation in 54.86 minutes) even though it was not maintained due to lack of energy dissipation in the simulation model. The decrease in angle is another indication of a negative rotation from the positive wheel torque, which is expected from the positive motor torque about the pitch axis.

Again, we see the equivalent dynamics with the quaternions (Figure 14). This time, note that  $q_3$ ,  $q_4$ , and  $\mu$  show complete spacecraft rotations instead of oscillations.

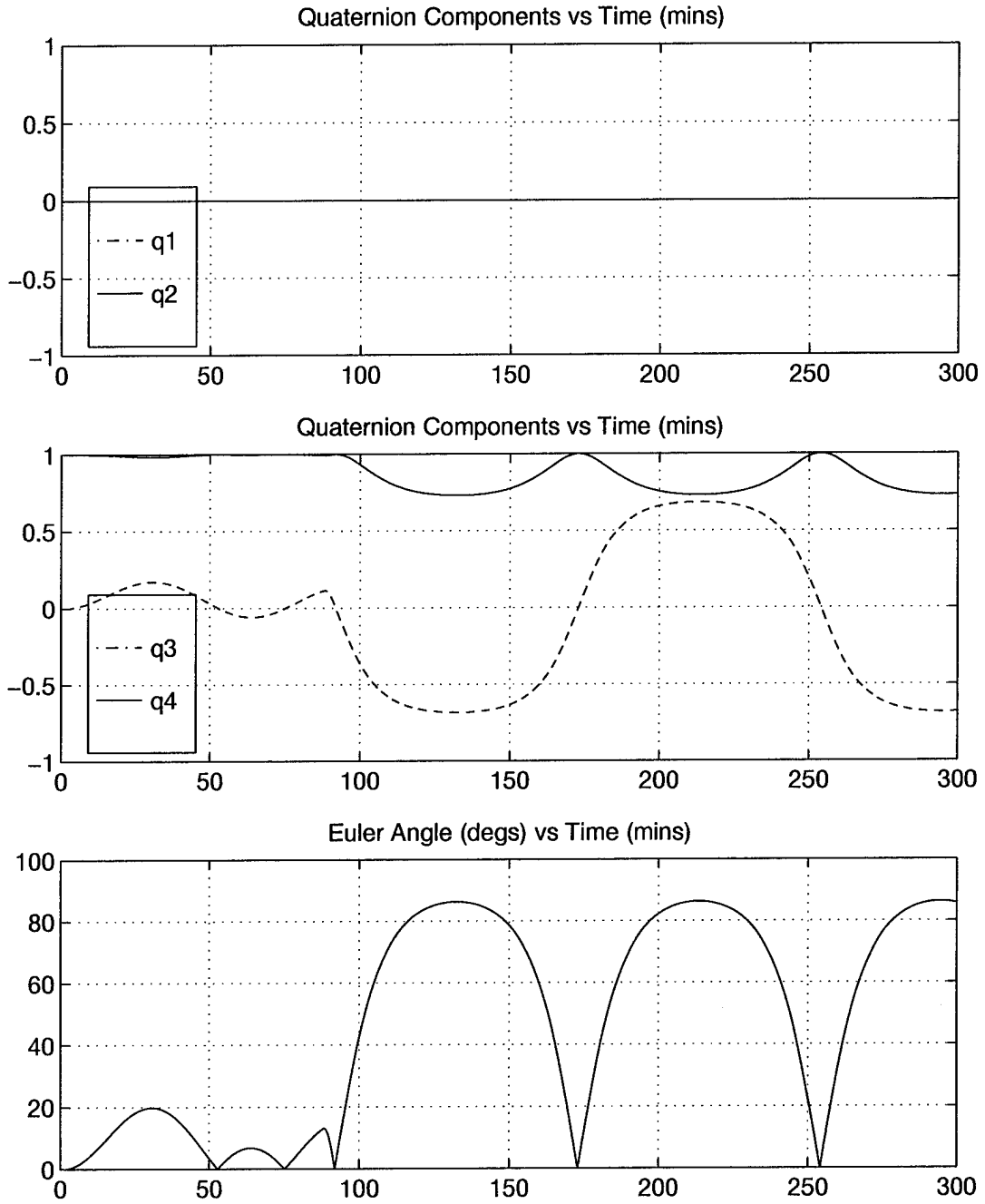


Figure 12. Lack of Inversion with Quaternions

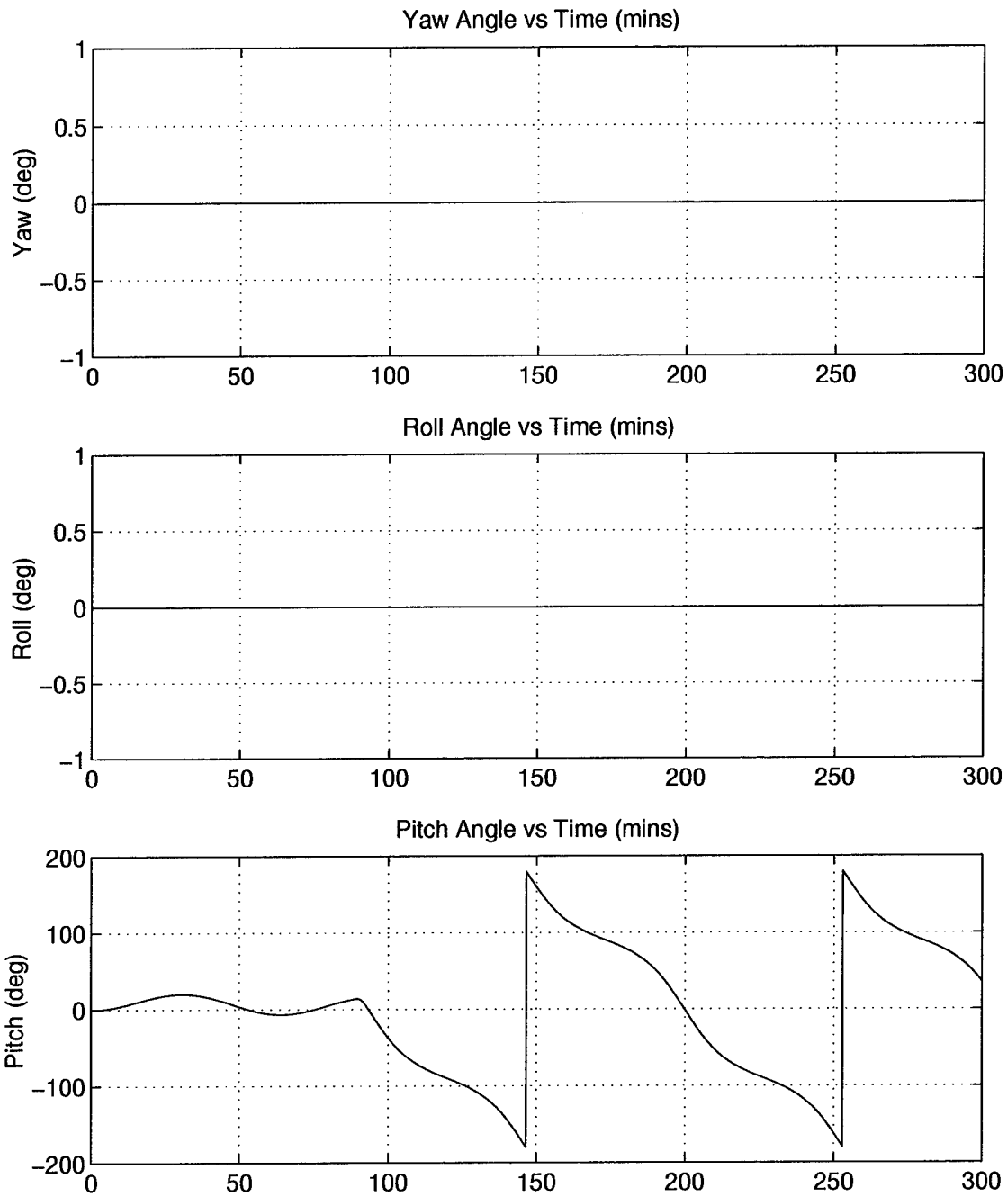


Figure 13. Spacecraft Inversion

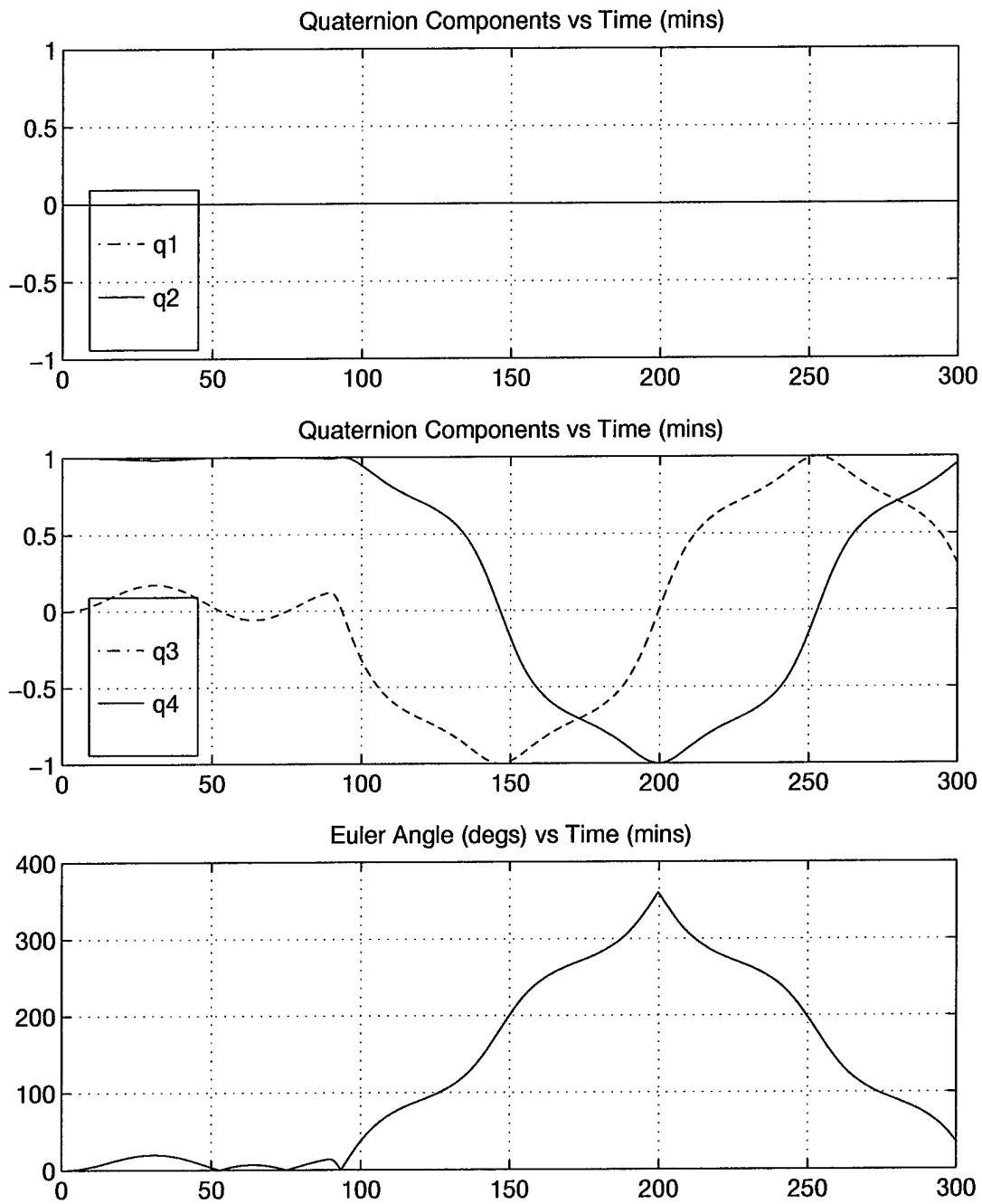


Figure 14. Spacecraft Inversion with Quaternions

### 5.3 *Pitch Angle Oscillations*

Having the magnitude of the motor torque greater than the maximum gravity-gradient torque is not the only requirement to invert the spacecraft as previously stated. It is the amount of angular impulse that dictates the inversion of the spacecraft. If the relationship between the angular impulse and its corresponding pitch oscillation angle can be developed, then a universal recovery algorithm can be developed. If the relationship were linear, then development of the algorithm would be simple. However, the relationship is not linear (Figure 15). The oscillation angles of the pitch axis do not increase correspondingly to an increase in angular impulse as shown in the plot of pitch oscillation angle verses wheel angular impulse. Similarly, if compared with the wheel despin times (the times of motor torque application), the oscillation angle does not correspondingly increase. A decrease in oscillation angle occurs despite an increase in angular impulse or a specific oscillation angle is reached from varying amounts of angular impulse (or despin times). For example, the pitch axis decreases in oscillation from the local maximum of  $73^\circ$  to the local minimum of  $52^\circ$  despite the increase in angular impulse. The local maximum and minimum occur after  $\approx 53$  and  $\approx 75$  minutes of wheel despin respectively. Recall that the pitch angle is  $0^\circ$  at these times during wheel despin. Furthermore, the pitch axis oscillates within  $60^\circ$  given 0.97 Nms, 1.38 Nms, and 1.59 Nms of angular impulse. This phenomenon, although unexpected, must be resolved before developing any recovery process.

However, once the angular impulse is sufficient to invert the spacecraft ( $\approx 1.68$  Nms), the amount of time taken to achieved attitude inversion decreases to a minimum of 24 minutes



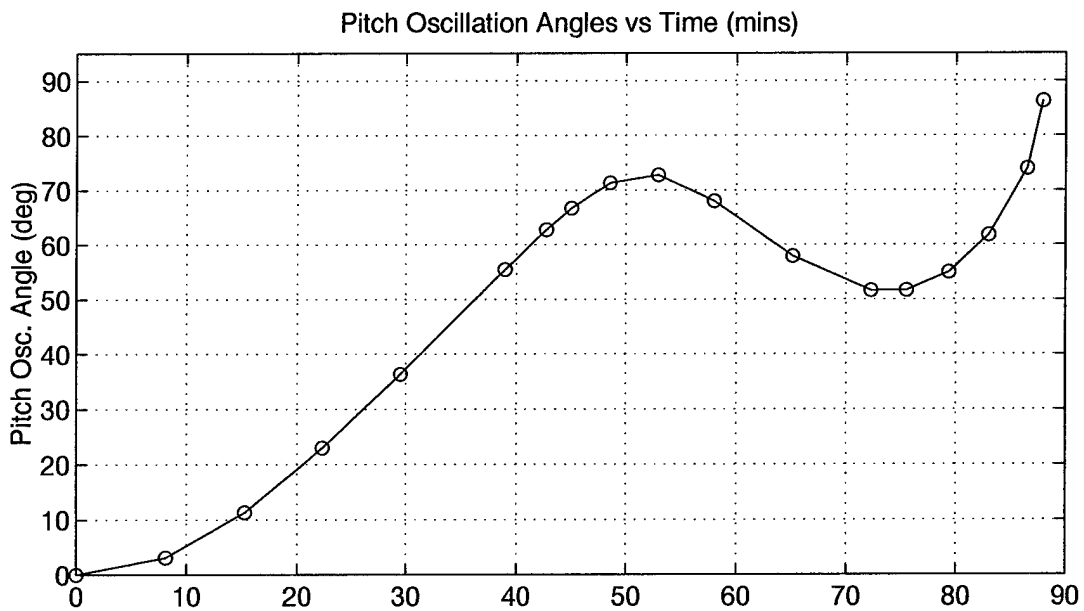
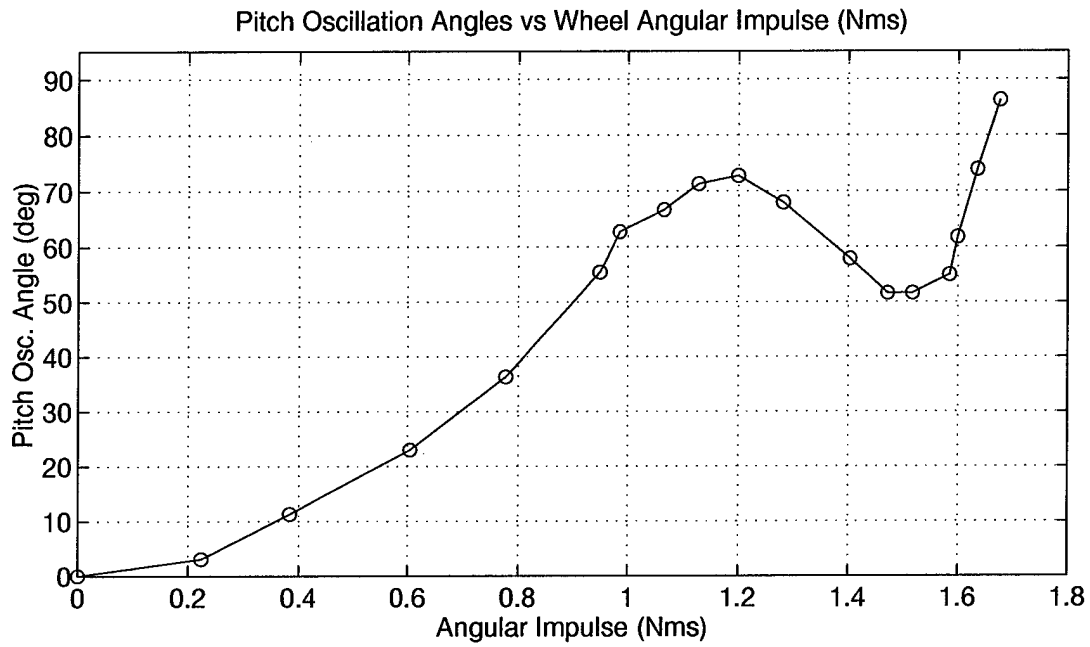


Figure 15. Non-Linear Pitch Oscillation Angle Relationship

at  $\approx 150$  minutes (Figure 16). Note that the angular impulse to re-invert Polar BEAR (1.676 Nms) from its anomalous motions is close to the angular impulse to invert the spacecraft in the pitch-axis only simulation. This indicates that the simplification of the spacecraft's motion about the pitch axis only is a good approximation. In other words, the additional motions about the roll and yaw axes do not appear to significantly affect the amount of angular impulse required to invert the spacecraft.

*5.3.1 Non-Linear Relationship.* One factor causing the decrease in oscillation angle, despite an increase in angular impulse, is the orientation of the spacecraft at the time the motor torque is applied. Recall that as the momentum wheel despins, the pitch angle oscillates through negative angles at times (Figure 11). If the motor torque is applied when the pitch angle is negative and further decreasing, then the resulting oscillation angle decreases as angular impulse increases. If the pitch angle is negative, but increasing, then the oscillation angle increases as angular impulse increases. If the pitch angle is zero, the corresponding oscillation angle is either the local maximum or minimum. These parameters are illustrated in Figure 17 and Table 1 where the motor torque is applied just before and just after zero pitch angle. For positive initial pitch angle, the resulting oscillation angle increases until the local maximum is reached then decreases once negative initial angles are reached. The oscillation angles continue to decrease to the local minimum before increasing again when positive initial angles are reached again. In other words, the application of a positive motor torque when the pitch rate is decreasing during wheel despin causes a reduction in the resulting oscillation angle. When the pitch rate increases again, the resulting oscillation angle increases.

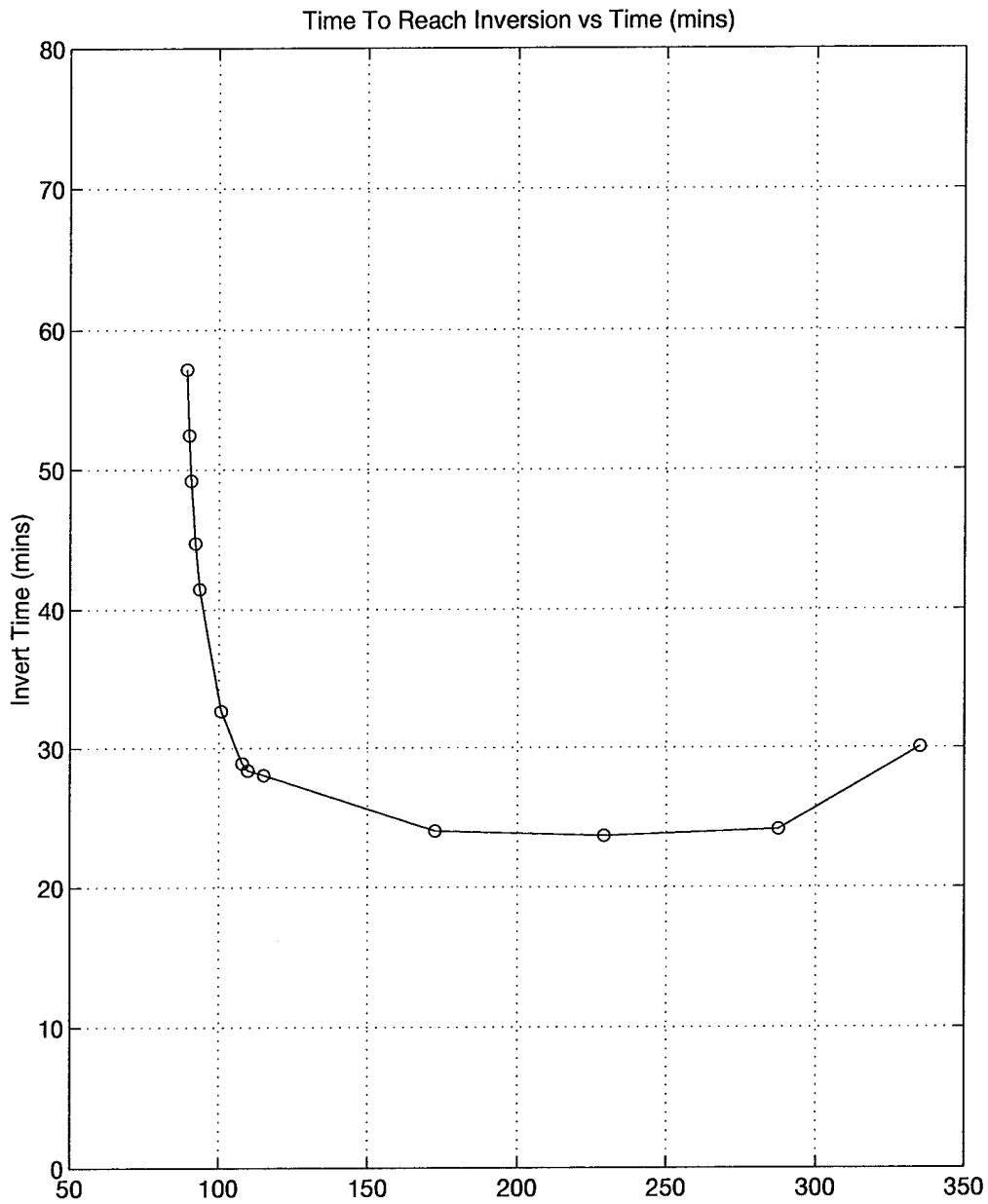


Figure 16. Time Until Inversion is Reached Given Wheel Despin Time

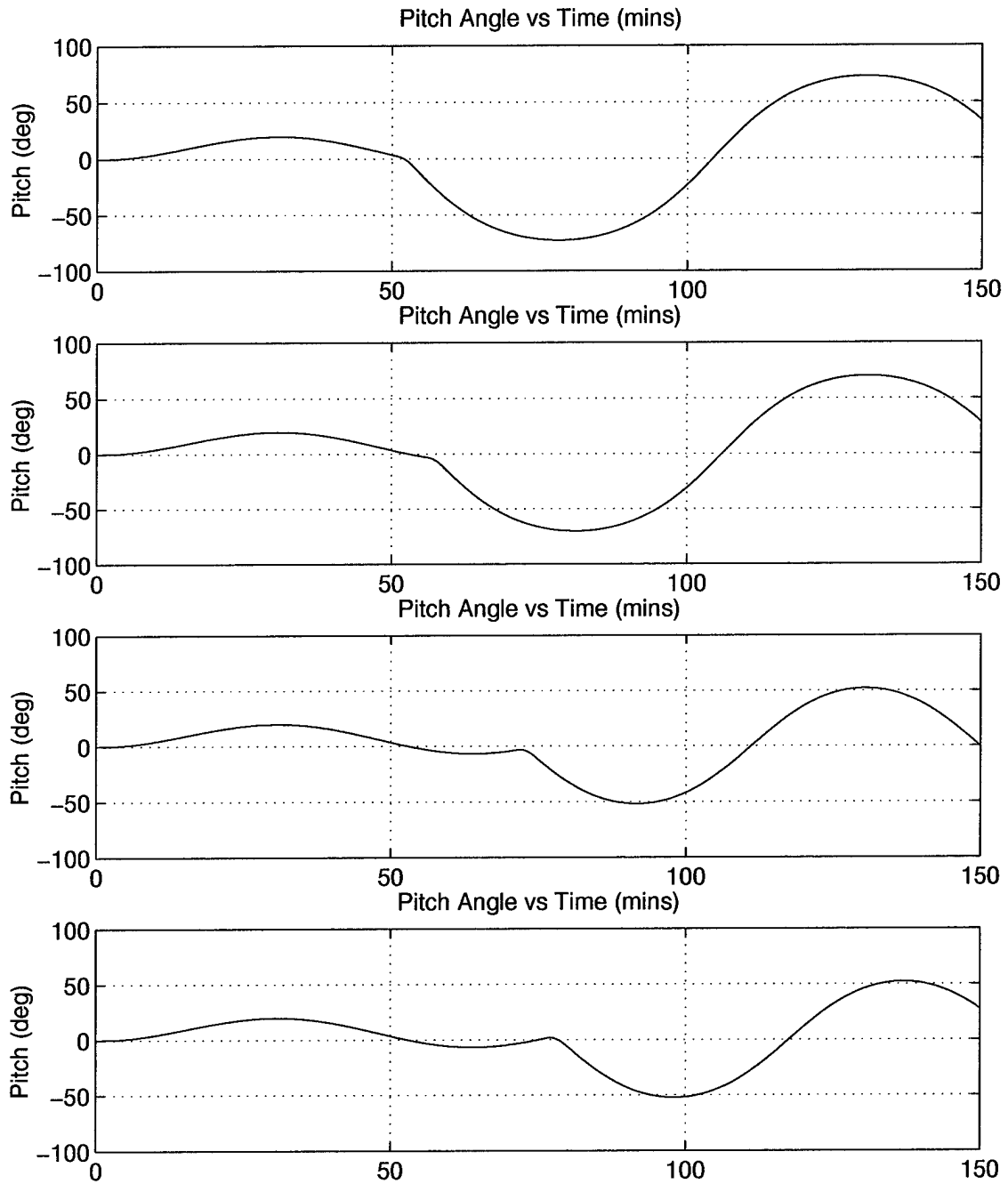


Figure 17. Pitch Oscillations about Local Points

Table 1. Results of Pitch Oscillation Angle about Local Inflection Points

Plot	Motor Torque Time	$\theta_p$ and $\dot{\theta}_p$	Oscillation Angle and Slope
1	51.1 minutes	$> 0^\circ$ , decreasing	$72.8^\circ$ , increasing
	52.8 minutes	$= 0^\circ$ , decreasing	$73^\circ$ , no slope (maximum)
2	56.2 minutes	$< 0^\circ$ , decreasing	$70.2^\circ$ , decreasing
3	71.5 minutes	$< 0^\circ$ , increasing	$52.8^\circ$ , decreasing
	75.2 minutes	$0^\circ$ , increasing	$52^\circ$ , no slope (minimum)
4	76.5 minutes	$> 0^\circ$ , increasing	$52.2^\circ$ , increasing

Another factor causing the non-linear phenomenon is the relationship between the inertia of the momentum wheel and that of the spacecraft. Even though the response of the spacecraft increases as the moment of inertia of the wheel increases, the relationship between the oscillation angle and the wheel despin time is still non-linear (Figure 18). For larger moments of inertia, we see the spacecraft returning to oscillatory motion as the wheel despin time increases even though it had already achieved inversion with lesser despin times. This behavior continues until the moment of inertia of the wheel is large enough to not cause oscillatory motions once inversion is achieved. For example, when  $I_w = 0.023 \text{ kgm}^2$ , the spacecraft no longer experiences oscillatory motions once inversion is achieved. This indicates that a minimum moment of inertia ratio between the wheel and spacecraft is required to have the resulting oscillation angle increase as the wheel despin time increases.

Similarly, when comparing the oscillation angle with the corresponding angular impulse produced from spinning up the wheel, the non-linear relationship exists (Figure 19). Here we see that spacecraft inversion is first achieved with an angular impulse of 1.22 Nms for all wheels with moments of inertia of  $\approx 0.013 \text{ kgm}^2$  or higher. This indicates that a gravity-gradient satellite is invertible with a minimum amount of angular impulse for any wheel

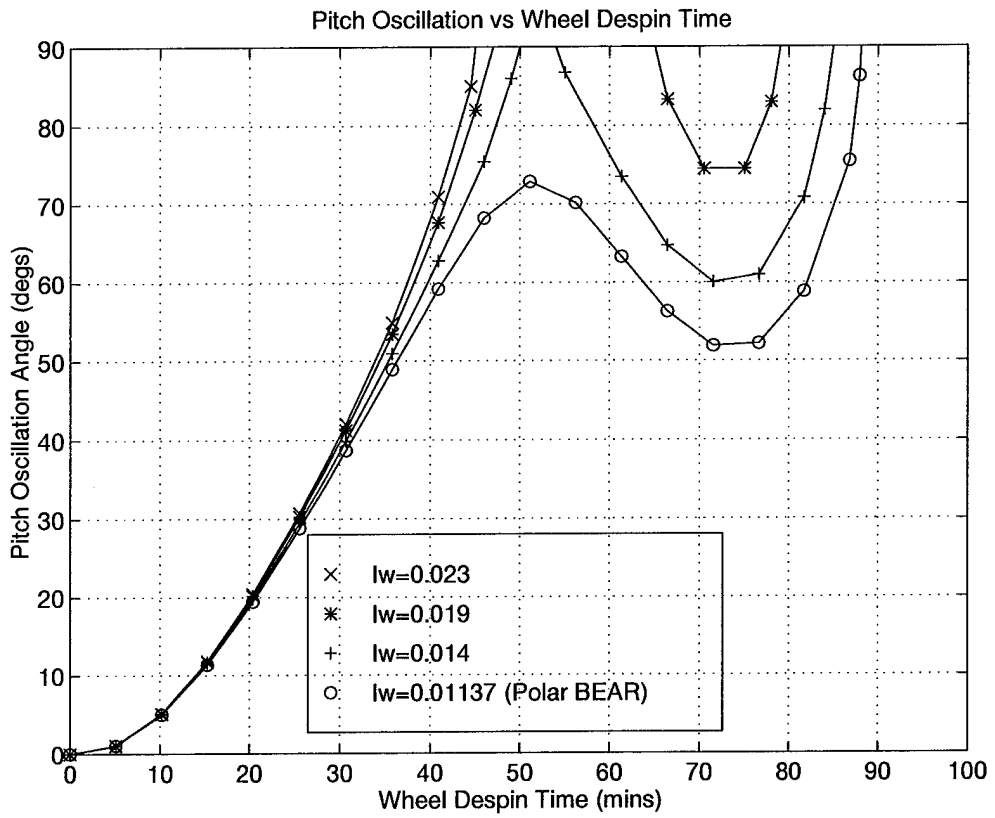


Figure 18. Pitch Oscillation and Wheel Despin Time Relationship

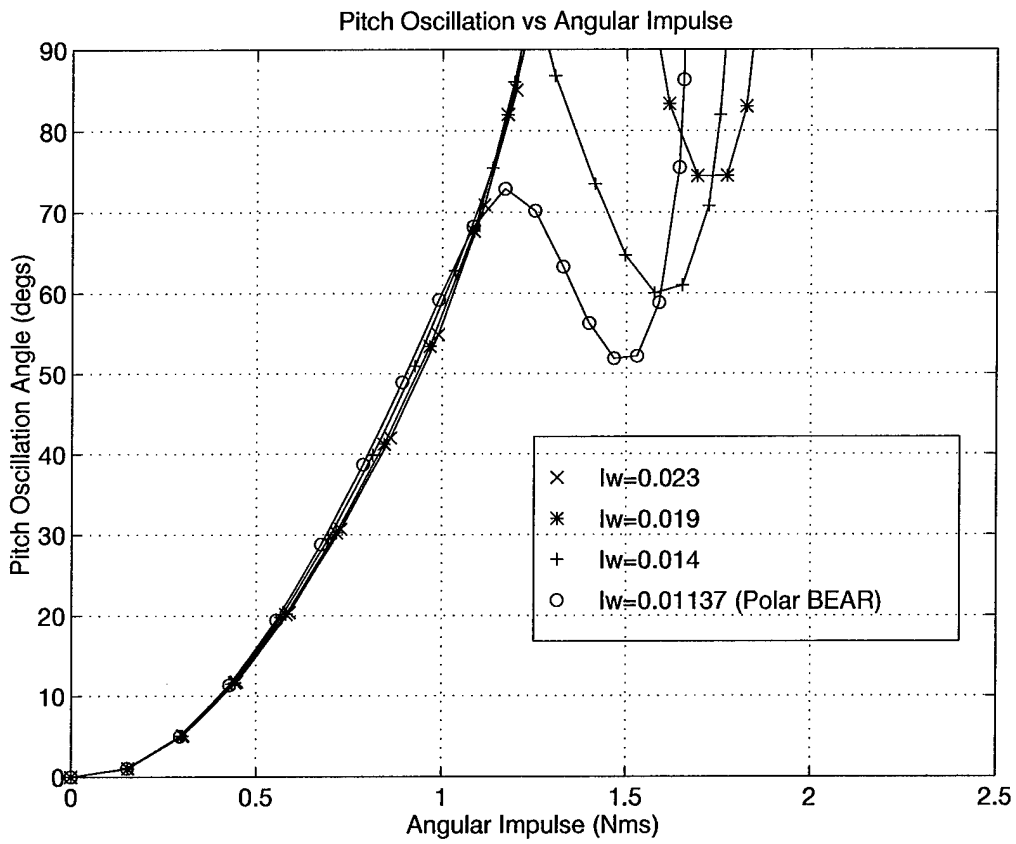


Figure 19. Pitch Oscillation and Angular Impulse Relationship

moment of inertia above a certain minimum. The minimum angular impulse only guarantees the inversion of the spacecraft, but not necessarily in the quickest time.

As expected, the relationship between the time it takes to reach inversion and the wheel despin time is also non-linear (Figure 20). We see the spacecraft returning to oscillatory motions for  $I_w < 0.023 \text{ kgm}^2$ . When  $I_w = 0.023 \text{ kgm}^2$ , a local minimum inversion time of

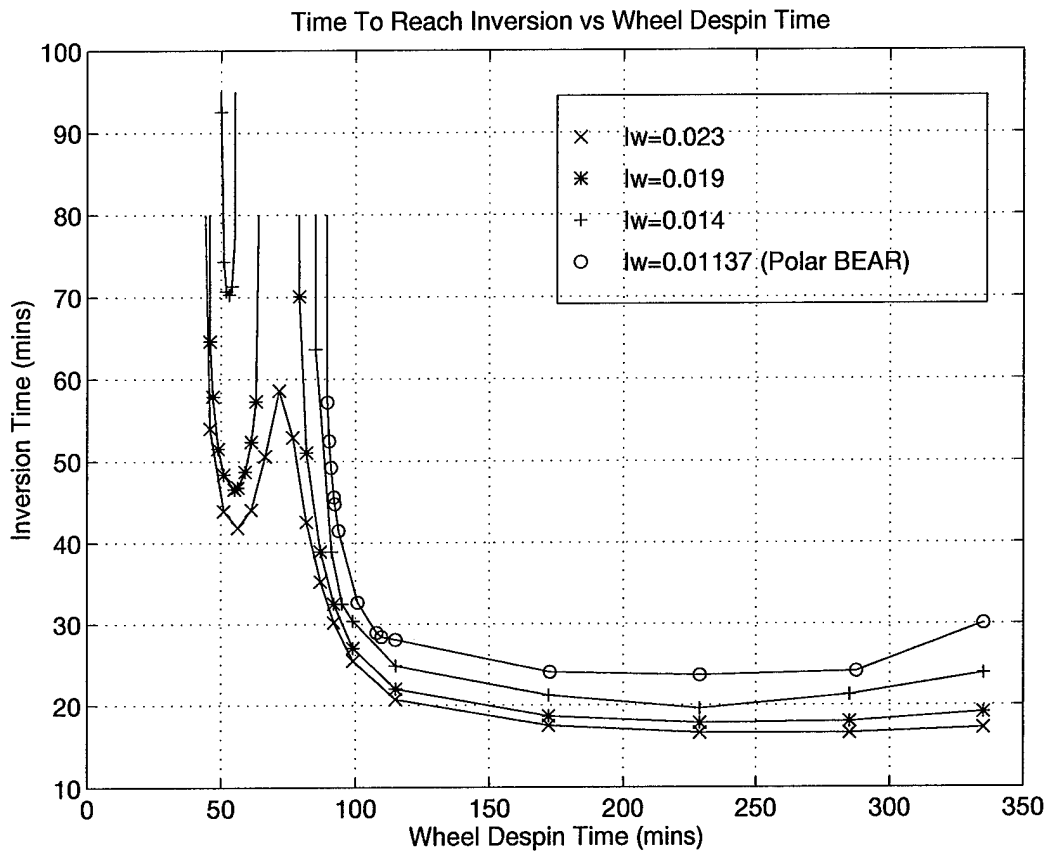


Figure 20. Time Until Inversion and Wheel Despin Time Relationship

42 minutes at  $\approx 57$  minutes of wheel despin exists. The local maximum is 58.5 minutes at  $\approx 74$  minutes of wheel despin. The angular impulse for the local minimum is 1.48 Nms as



illustrated in Figure 21. Here, the local minimum is the shortest amount of time it takes to invert the satellite with the least amount of angular impulse expended.

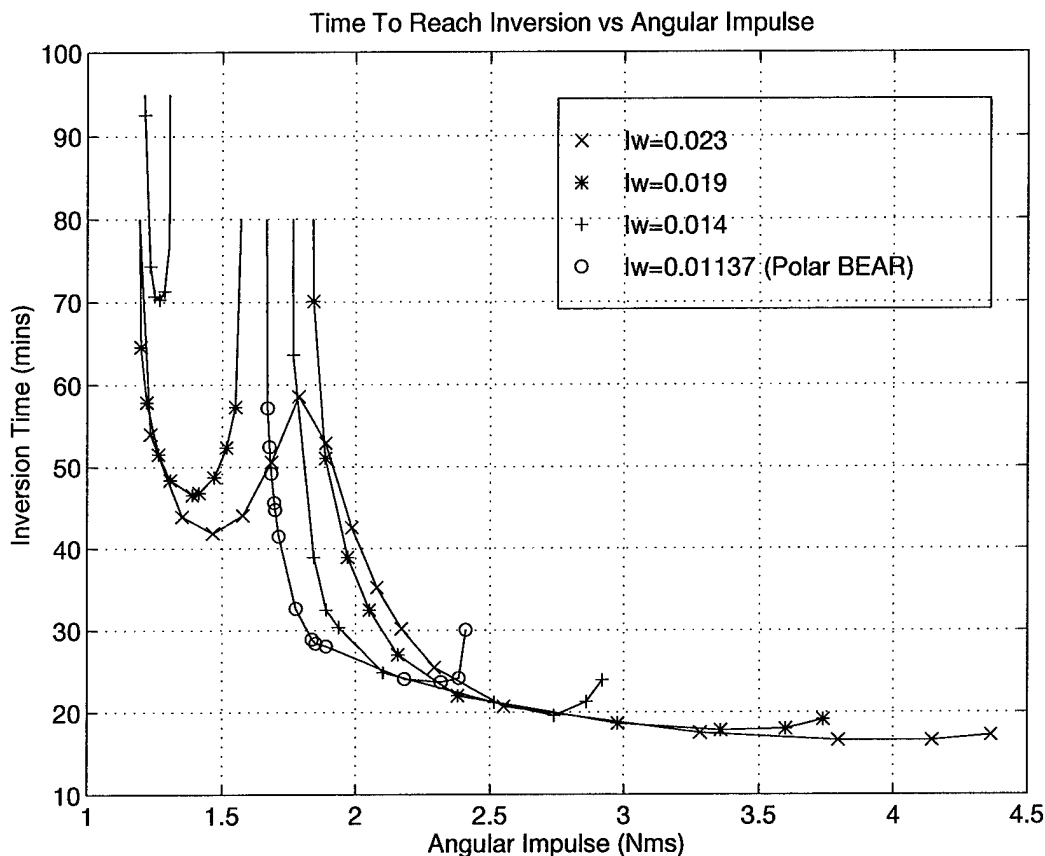


Figure 21. Time Until Inversion and Angular Impulse Relationship

The location of the pitch angle at the time of motor torque application for  $I_w = 0.023$   $\text{kgm}^2$  is illustrated in Figure 22. Again we see that the times of the local minimum and maximum (57 and 74 minutes respectively) occur when the pitch angle is  $0^\circ$  when the motor torque is applied. This indicates that for a wheel to spacecraft moment of inertia ratio above a certain minimum, the quickest time to reach inversion with the least amount of energy expended is attainable when the pitch angle during despinning of the wheel is first  $0^\circ$ .

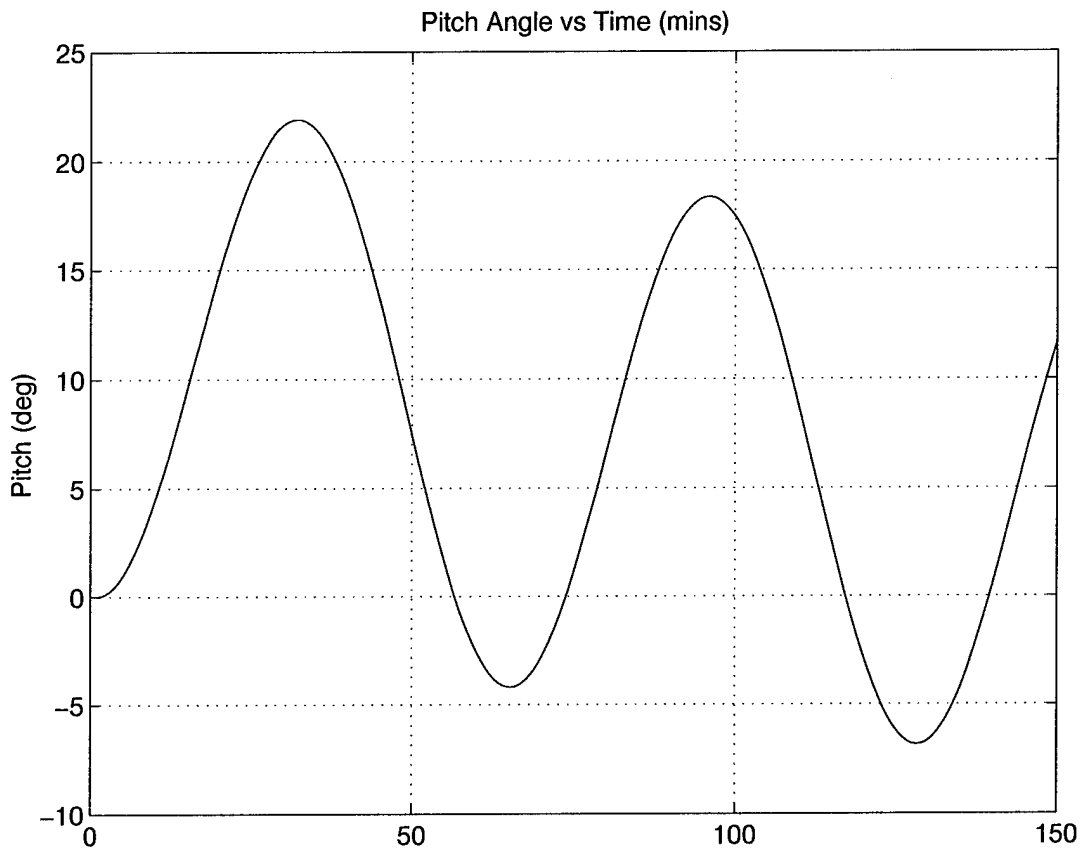


Figure 22. Despin Pitch Motion for Wheel Mass Inertia of  $0.023 \text{ kgm}^2$

It is also important to note that the local maximum and minimum occur only for the first set of negative pitch angles. Recall that this was also the case for the previous local maximum and minimum points of the original wheel moment of inertia of Polar BEAR. In both cases, the subsequent negative pitch angles no longer significantly affects the dynamics of the spacecraft after inversion is achieved.

## *VI. Conclusions and Recommendations*

The purpose of this research was to explain the process by which the Polar BEAR gravity-gradient satellite recovered from its anomalous motions. From this analysis, an algorithm for attitude inversion of similar satellites with the momentum wheel was sought through the motions of spacecraft about the pitch axis only.

### *6.1 Conclusions*

*6.1.1 Re-inversion.* The re-inversion of the Polar BEAR satellite was successfully accomplished in our simulation process. Although all attitude control and motion damping devices of the Polar BEAR satellite were not modelled and utilized for attitude inversion, the effectiveness of the momentum wheel as the sole attitude inversion mechanism was demonstrated. Attitude inversion was achieved when the momentum wheel was allowed to despin for an orbit in the simulation as it was in the actual re-inversion of Polar BEAR in 1987. This subsequently enabled the spin-up motor torque to provide an impulsive torque large enough to rotate the spacecraft through an equilibrium configuration where no gravity-gradient torques were induced. Furthermore, the rotation was mostly a negative rotation about the pitch axis given the positive motor torque on that axis. The re-inversion process finished with the satellite oscillating about all three axes, although not within the oscillation angles of the actual re-inversion process. This is attributed to the lack of energy dissipation in the simulation model.

*6.1.2 Pitch-Only Motion.* The pitch-only motions of a spacecraft produced an unexpected non-linear relationship between the oscillation angles of the pitch axis and the wheel despin time. The impulsive torque on the wheel induced oscillations that did not linearly increase as the angular impulse from the wheel (or the wheel despin time) increased. This phenomenon in part is attributed to the value of the pitch angle during wheel despin. If the spin-up motor torque is applied when the pitch angle is  $0^\circ$  or less, the oscillation angle decreases even though the angular impulse from the wheel increases. When the pitch angle increases back to positive angles during wheel despin, the oscillation angles increase also until spacecraft inversion is achieved. Inversion is achieved when the angular impulse is large enough to rotate the spacecraft through the  $90^\circ$  unstable configuration. Subsequently, the amount of time it takes for inversion to be reached linearly decreases to a minimum as wheel despin time increased. Obtaining this minimum requires a large expenditure of angular impulse.

Another factor involved in the phenomenon is the relationship between the moment of inertia of the wheel to that of the spacecraft. If the wheel to spacecraft moment of inertia is above a certain minimum, then the spacecraft no longer experiences oscillatory motions once inversion is achieved with a lesser amount of angular impulse. Given the same wheel moment of inertia quantities, the relationship between the time until inversion is reached and the wheel despin time is also non-linear. Instead, a local minimum, indicating the shortest inversion time with the least amount of angular impulse, occurs. This minimum occurs when the pitch angle is  $0^\circ$  during the despinning of the wheel and the motor torque is applied. The dynamics

described above for both non-linear cases only occur for the first set of negative pitch angles during wheel despin. For the intermediate wheel moments of inertia, the dynamics of the spacecraft do not appear to be affected by initial pitch angles at the time of motor torque application.

*6.1.3 Universal Recovery Algorithm.* The universal attitude inversion process for gravity-gradient satellites through application of a momentum wheel torque was not completely obtained in this research thesis. However, two conditions are relevant in the recovery process: the wheel to spacecraft moment of inertia ratio and the pitch angle at the time of wheel spin-up. For the former condition, if the inertia ratio is above a certain minimum, the optimal time to spin-up the wheel is when the pitch angle is first at  $0^\circ$  during wheel despin. Application of the motor torque at that time results in a minimum spacecraft inversion time with the least amount of energy expended.

## *6.2 Recommendations*

Further analysis for the optimal parameters of the recovery process is required, in particular, the minimum angular impulse required to invert the spacecraft given any inertia ratio. Developing a mathematical formula that would define this parameter would in turn define the required despin time of the wheel. Furthermore, additional analysis of the inversion process with roll and yaw motions or with other attitude control devices would also be beneficial for the development of the universal recovery algorithm.

## Bibliography

1. Chobotov, Vladimir A. *Spacecraft Attitude Dynamics and Control*. Malabar, Florida: Krieger Publishing Company, 1991.
2. Hughes, Peter C. *Spacecraft Attitude Dynamics*. New York: John Wiley and Sons, Inc., 1986.
3. Hunt, John W. "Senior Staff Engineer, Space Department, Johns Hopkins University Applied Physics Laboratory." Electronic Mail Interview, 1995.
4. Hunt, John W. and J. C. Ray. "Flexible Booms, Momentum Wheels, and Subtle Gravity-Gradient Instabilities." in *Proceedings of the AIAA Space Programs and Technologies Conference*, March 24-27, 1992, Huntsville AL.
5. Hunt, John W. and Charles E. Williams. "Anomalous Attitude Motion of The Polar BEAR Satellite," *Johns Hopkins APL Technical Digest*, 8(3):324-328 (1987).
6. Kaplan, Marshall H. *Modern Spacecraft Dynamics and Control*. New York: John Wiley and Sons, 1976.
7. Nayfeh, Ali H. and Dean T. Mook. *Nonlinear Oscillations*. New York: John Wiley and Sons, 1979.
8. Peterson, Max R. and David G. Grant. "The Polar BEAR Spacecraft," *Johns Hopkins APL Technical Digest*, 8(3):295-302 (1987).
9. Wertz, James R., editor. *Spacecraft Attitude Determination and Control*. Boston: D. Reidel Publishing Company, 1978.
10. Wiesel, William E. *Spaceflight Dynamics*. New York: McGraw-Hill Book Company, 1989.

## *Vita*

1Lt Jules-Francois D. Desamours was born on 18 December 1969 in Brooklyn, New York. He graduated from Essex Catholic Boys High School in 1987 and entered undergraduate studies at the United States Air Force Academy in 1988. He graduated with a Bachelor of Science degree in Astronautical Engineering and received his commission on 27 May 1992. His first assignment was at Wright-Patterson AFB as a space mission control analyst. In May 1994, he entered the School of Engineering, Air Force Institute of Technology.

Permanent address: 329 Gait Court  
Kissimmee, Florida 34744



# REPORT DOCUMENTATION PAGE

Form Approved  
OMB No. 0704-0188

Public reporting burden for this collection of information is estimated to average 1 hour per response, including the time for reviewing instructions, searching existing data sources, gathering and maintaining the data needed, and completing and reviewing the collection of information. Send comments regarding this burden estimate or any other aspect of this collection of information, including suggestions for reducing this burden, to Washington Headquarters Services, Directorate for Information Operations and Reports, 1215 Jefferson Davis Highway, Suite 1204, Arlington, VA 22202-4302, and to the Office of Management and Budget, Paperwork Reduction Project (0704-0188), Washington, DC 20503.

<b>1. AGENCY USE ONLY (Leave blank)</b>	<b>2. REPORT DATE</b> December 1995	<b>3. REPORT TYPE AND DATES COVERED</b> Master's Thesis
---	--	--

<b>4. TITLE AND SUBTITLE</b> ANALYSIS OF GRAVITY-GRADIENT SATELLITE ATTITUDE INVERSION	<b>5. FUNDING NUMBERS</b>
---	---------------------------

<b>6. AUTHOR(S)</b> Jules-Francois D. Desamours	
--	--

<b>7. PERFORMING ORGANIZATION NAME(S) AND ADDRESS(ES)</b> Air Force Institute of Technology, WPAFB OH 45433-6583	<b>8. PERFORMING ORGANIZATION REPORT NUMBER</b> AFIT/GSO/ENY/95D-02
---	--

<b>9. SPONSORING/MONITORING AGENCY NAME(S) AND ADDRESS(ES)</b> Maj David Vallado PL/VTA 3550 Aberdeen Ave SE Kirtland AFB, NM 87117-5776	<b>10. SPONSORING/MONITORING AGENCY REPORT NUMBER</b>
--	---

**11. SUPPLEMENTARY NOTES**

<b>12a. DISTRIBUTION/AVAILABILITY STATEMENT</b> Distribution Unlimited	<b>12b. DISTRIBUTION CODE</b>
---	-------------------------------

**13. ABSTRACT (Maximum 200 words)**

The purpose of this research is to understand and describe the process by which the 1986 Polar BEAR gravity-gradient research satellite of John Hopkins University/Applied Physics Laboratory achieved an orbital attitude correction (re-inversion) from an inverted orientation through the utilization of its momentum wheel. Understanding this process provides an analytical foundation from which a universal attitude inversion process for other gravity-gradient satellites with similar anomalous motions may be sought and developed. The equations of motion for a gravity-gradient satellite with a momentum wheel are derived and implemented in FORTRAN for simulation of the dynamics of the spacecraft. Several re-inversion characteristics are observed, in particular, the dynamics about the pitch axis. The resulting observations demonstrate an unexpected non-linear relationship between the oscillation angle of the pitch axis and the despin time of the momentum wheel. This phenomenon depends in part on the size of the momentum wheel compared to that of the spacecraft and on the pitch angle at the time of motor torque application.

<b>14. SUBJECT TERMS</b> Gravity-Gradient Satellite, Momentum Wheel, Attitude Inversion	<b>15. NUMBER OF PAGES</b> 56
	<b>16. PRICE CODE</b>

<b>17. SECURITY CLASSIFICATION OF REPORT</b> UNCLASSIFIED	<b>18. SECURITY CLASSIFICATION OF THIS PAGE</b> UNCLASSIFIED	<b>19. SECURITY CLASSIFICATION OF ABSTRACT</b> UNCLASSIFIED	<b>20. LIMITATION OF ABSTRACT</b> UL
--	---	--	---